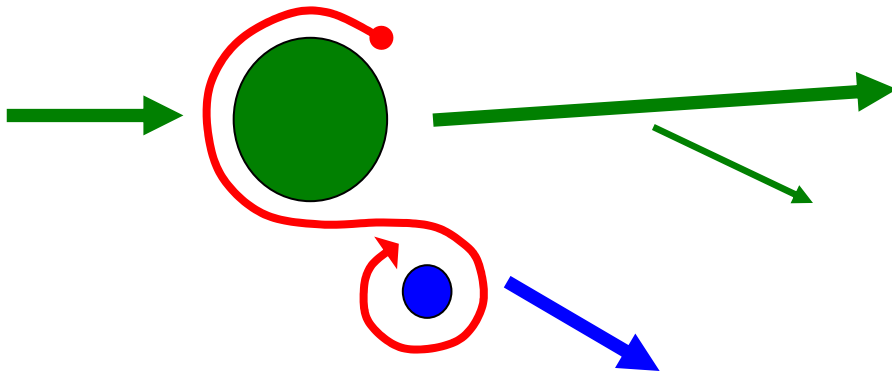


Transfer reactions in Inverse Kinematics

*

an experimental overview

Nucleon Transfer with Radioactive Beams



- focus on 10-30 MeV/A reactions
- kinematics are then generic
- a general array can be envisaged
- resolution issues are general
- three classes of solution/choice
- catalyst to discussion
- outline of TIARA array

- overview : Nucl Phys A701 (2002) 1c-6c
- overview : Acta Phys Pol 32B (2001) 1049-1060
- resolution : JSW et al NIM A396 (1997) 147-164

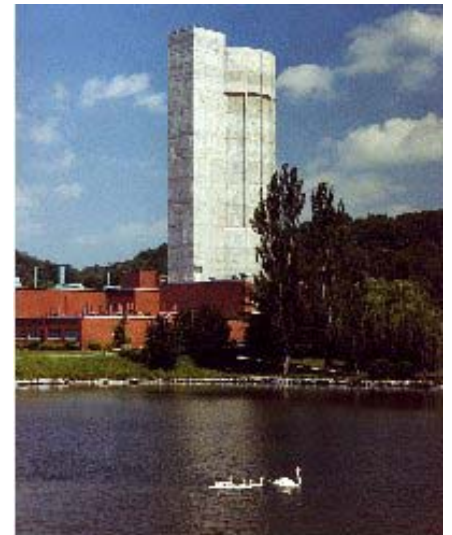
Uni**S**

University of Surrey

Wilton Catford

w.catford@surrey.ac.uk

Oak Ridge TN
June 2002



Velocity vector addition diagram

Particles exit close to 90 degrees

lab
 V_{light}

forward scattered target particle in c.m. frame

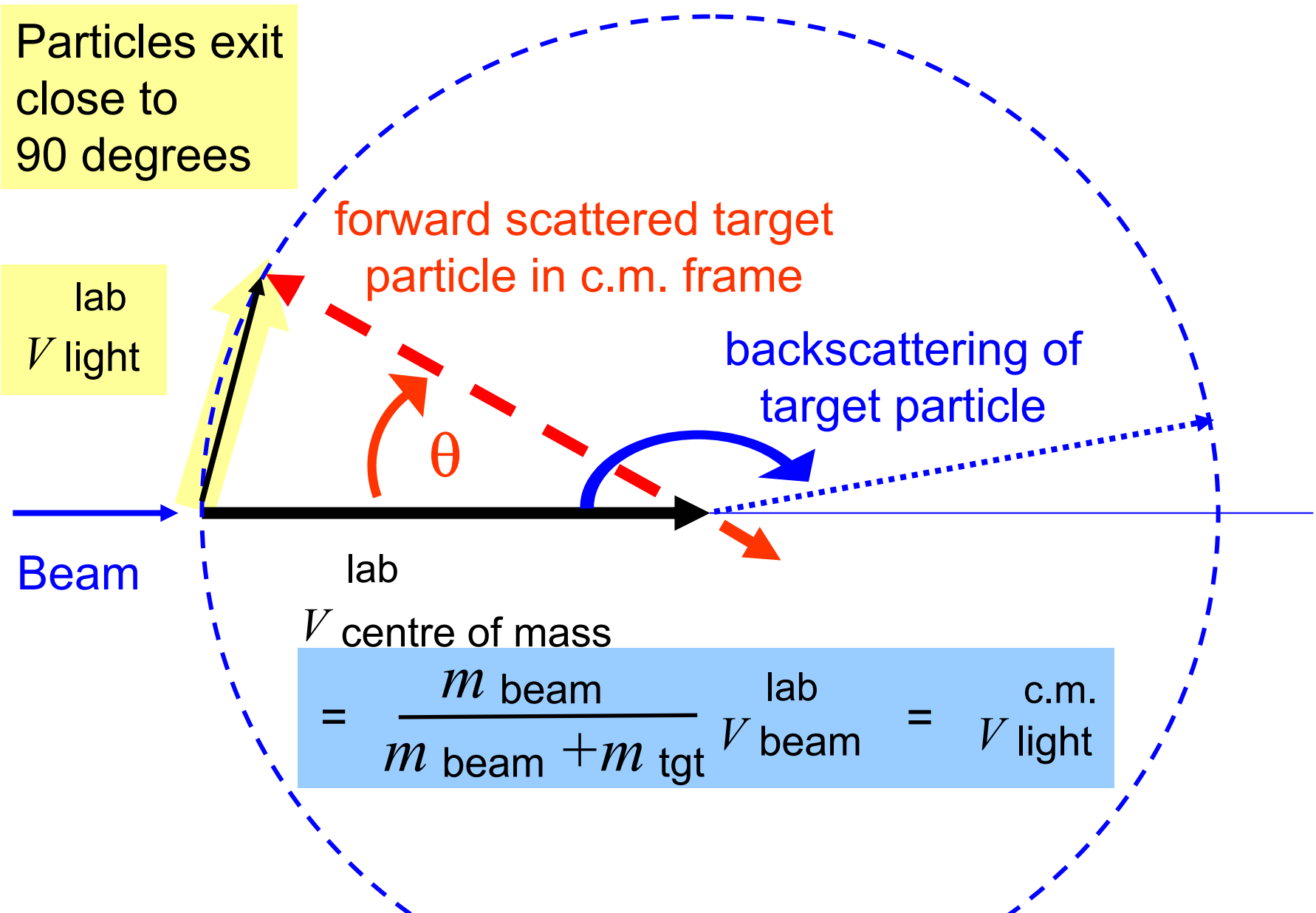
backscattering of target particle

Beam

lab

$V_{\text{centre of mass}}$

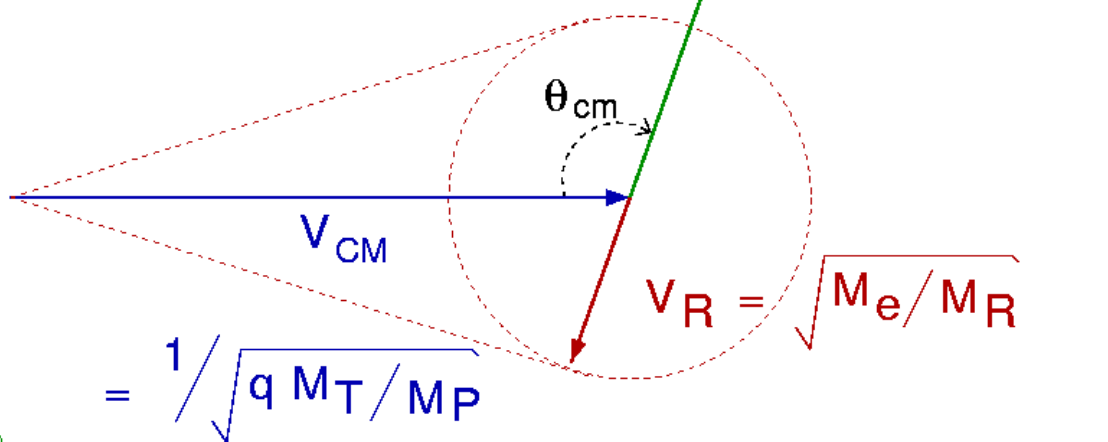
$$= \frac{m_{\text{beam}}}{m_{\text{beam}} + m_{\text{tgt}}} V_{\text{beam}} = V_{\text{light}}$$



Velocity Addition

(non-relativistic)

Reaction:
 $T(P, e)R$



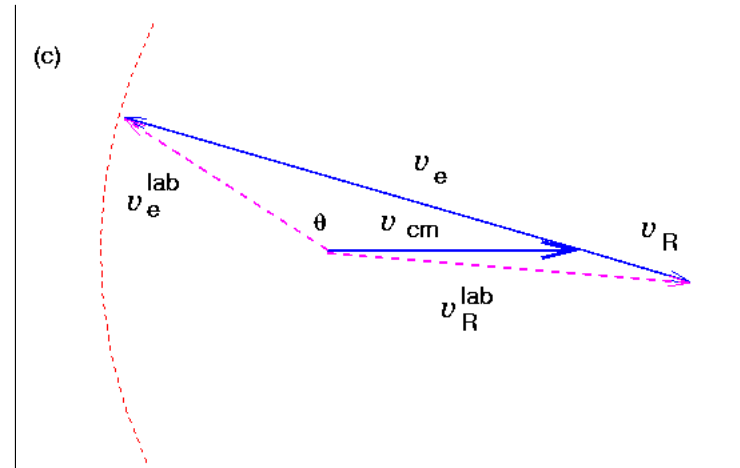
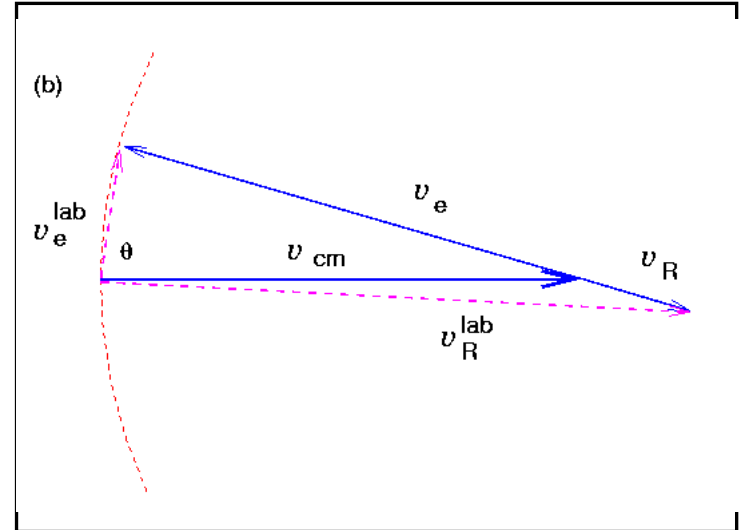
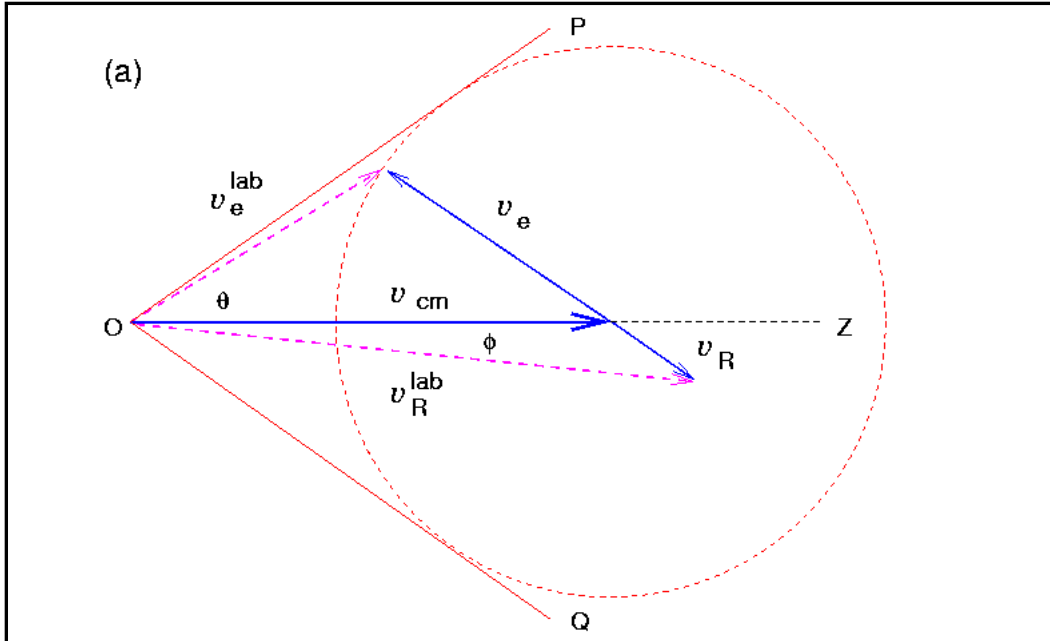
$$q = 1 + \frac{Q_{gs} - E_x}{E_{CM}}$$

$$V_{unit} = \sqrt{2 q E_{CM} / [M_R + M_e]}$$

$$q \cong 1 + Q_{\text{tot}} / (E/A)_{\text{beam}}$$

$$f = 1/2 \text{ for (p,d), } 2/3 \text{ for (d,t)}$$

Inverse Kinematics



$$\frac{v_e}{v_{\text{cm}}} = \left(q f \frac{M_R}{M_P} \right)^{1/2} \cong \sqrt{q f}$$

$$\theta_{\text{max}} = \sin^{-1} \sqrt{f}$$

v_{cm} is the velocity of the centre of mass, in the laboratory frame

Reaction Q-values in MeV

Z



Ne				14	15	16	17	18	19	20	21	22	23	24	25	26	27	28	29	30
						-77.6	-13.4	-17.0	-9.4	-14.6	-4.5	-8.1	-3.0	-6.6	-2.0	-3.3	0.1	-1.5	2.5	-2.1
F				13	14	15	16	17	18	19	20	21	22	23	24	25	26	27	28	29
					-81.1	-22.7	-11.9	-14.6	-6.9	-8.2	-4.4	-5.9	-3.0	-5.3	-1.4	-2.7	0.9	2.5	1.8	
O				12	13	14	15	16	17	18	19	20	21	22	23					
					-14.8	-21.0	-11.0	-13.4	-1.9	-5.8	-1.7	-5.4	-1.6	-4.5	-0.7					
N				11	12	13	14	15	16	17	18	19	20	21						
					-20.7	-13.4	-17.8	-8.3	-8.6	-0.3	-3.7	-0.6	-3.1	0.2	-2.6					
C	8	9		10	11	12	13	14	15	16	17	18	19	20						
					-12.0	-19.1	-10.3	-16.5	-2.7	-6.0	1.0	-2.0	1.5	-2.0	1.9	-1.4				
B	7	8	9		10	11	12	13	14	15										
					-10.8	-16.4	-6.2	-9.2	-1.1	-2.7	1.3	-0.5								
Be	6	7	8		9	10	11	12	13	14										
					-8.5	-16.7	0.6	-4.6	1.7	-0.9	4.1	-0.7								
Li	4	5	6	7	8	9	10													
					-13.3	-3.4	-5.0	0.2	-1.8	3.0										

↑ N=20

↑ N=14

↑ N=8

□ = stable

Reaction Q-value in MeV

(p, d): refer to cell of TARGET

(d, p): (-1) x (Cell of PRODUCT)

(d, t): Cell of TARGET + 4.0 MeV



N

Ne					15	16	17	18	19	20	21	22	23	24	25	26	27	28	29	30
					60.3	5.4	4.0	1.6	-0.9	-7.4	-7.5	-9.8	-9.8	-11.1	-11.6	-12.3	-13.1	-17.1	-16.4	-18.4
F				13	14	15	16	17	18	19	20	21	22	23	24	25	26	27	28	29
					75.0	8.7	7.0	6.0	4.9	-0.1	-2.5	-5.1	-5.6	-7.0	-7.9	-8.6	-9.6	-16.7	-14.1	-15.6
O				12	13	14	15	16	17	18	19	20	21	22	23					
					5.4	4.0	0.9	-1.8	-6.6	-8.3	-10.4	-11.6	-13.9	-15.6	-17.5	-19.0				
N				11	12	13	14	15	16	17	18	19	20	21						
					7.3	4.9	3.6	-2.1	-4.7	-6.0	-7.6	-9.7	-10.8	-12.5	-13.7					
C	8	9		10	11	12	13	14	15	16	17	18	19	20						
					5.4	4.2	1.5	-3.1	-10.5	-12.0	-15.3	-15.6	-17.1	-17.9	-20.2	-21.4	-24.1			
B	7	8	9		10	11	12	13	14	15										
					7.7	5.4	5.7	-1.1	-5.7	-8.6	-10.3	-13.1	-12.9							
Be	6	7	8		9	10	11	12												
					4.9	-0.1	-11.8	-11.4	-14.1	-15.5	-17.6									
Li	4	5	6	7	8	9	10													
					8.4	7.5	0.9	-4.5	-7.0	-8.4	-8.7									

↑ N=20

↑ N=14

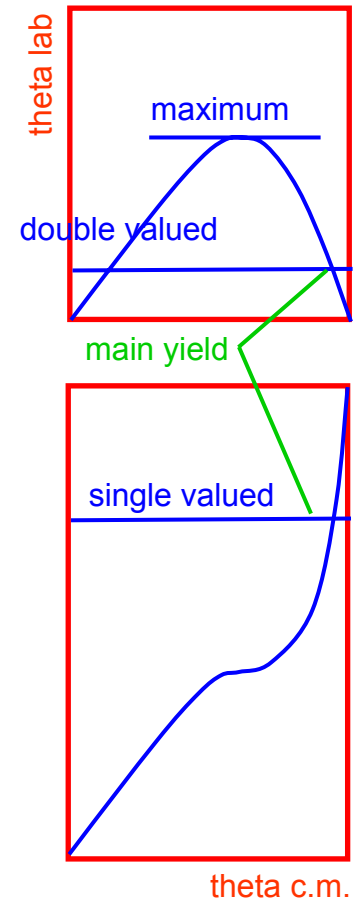
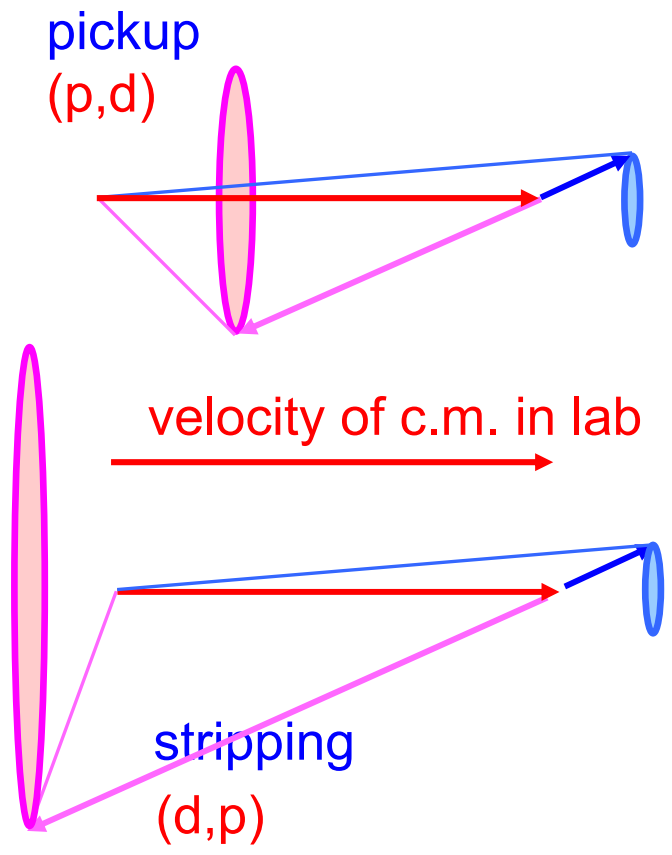
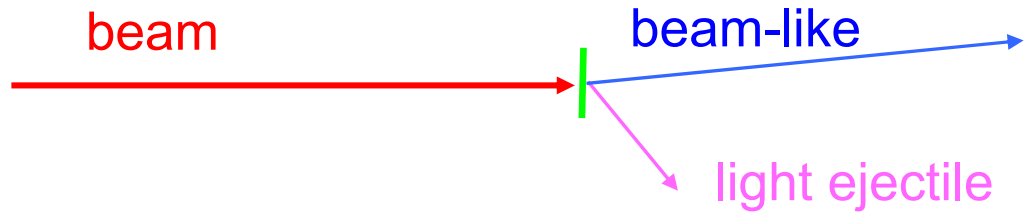
↑ N=8

□ = stable

Reaction Q-value in MeV

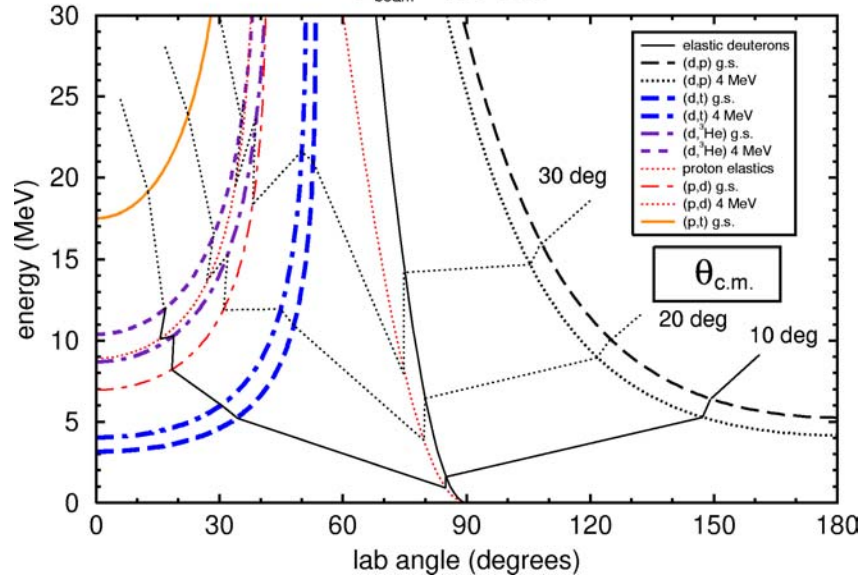
(d, ³He): refer to cell of TARGET

Kinematics of nucleon transfer in inverse kinematics



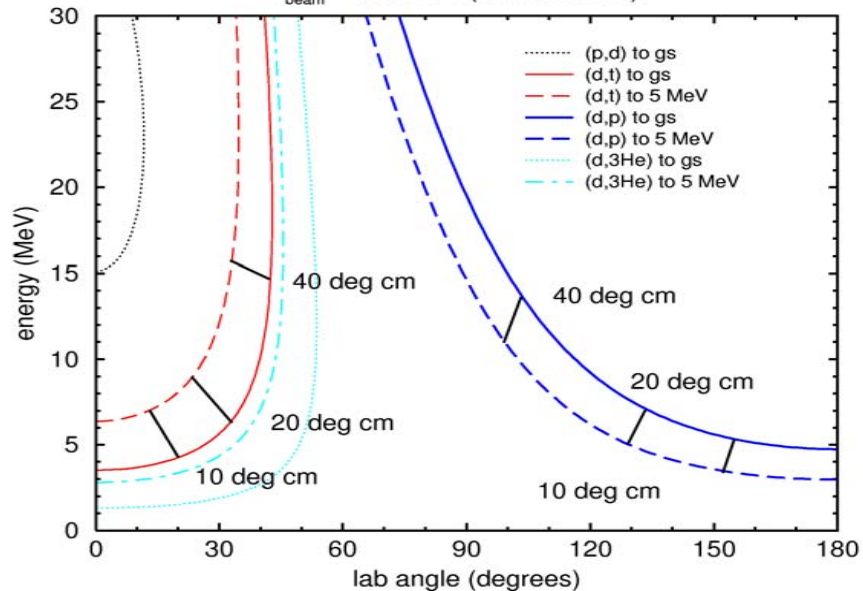
^{16}C incident on ^2H at 35 MeV/u

$E_{\text{beam}} = 560 \text{ MeV}$



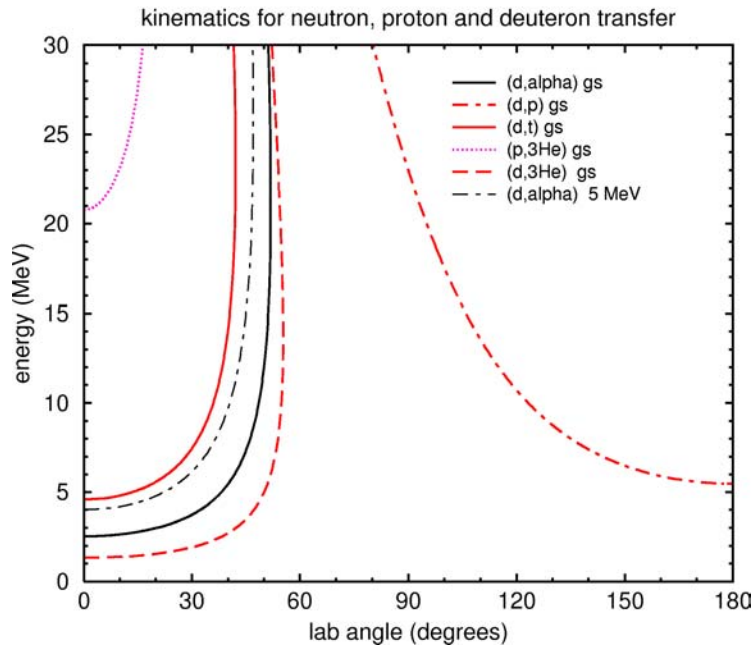
(p,d) and (d,t) and (d,p) on ^{74}Kr in inverse kinematics

$E_{\text{beam}} = 900 \text{ MeV} (12.16 \text{ MeV/A})$

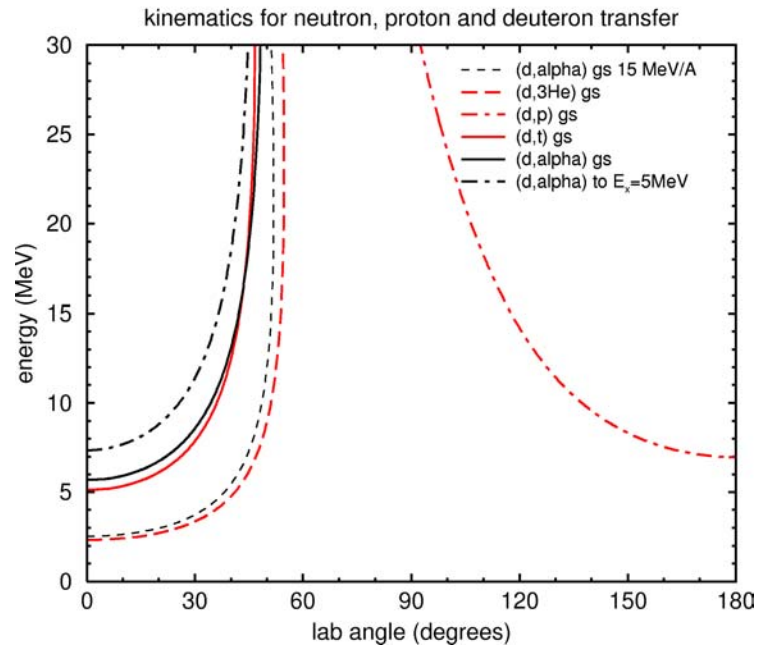


The general form of the kinematic diagrams is determined by the light particle masses, and has little dependence on the beam mass or velocity

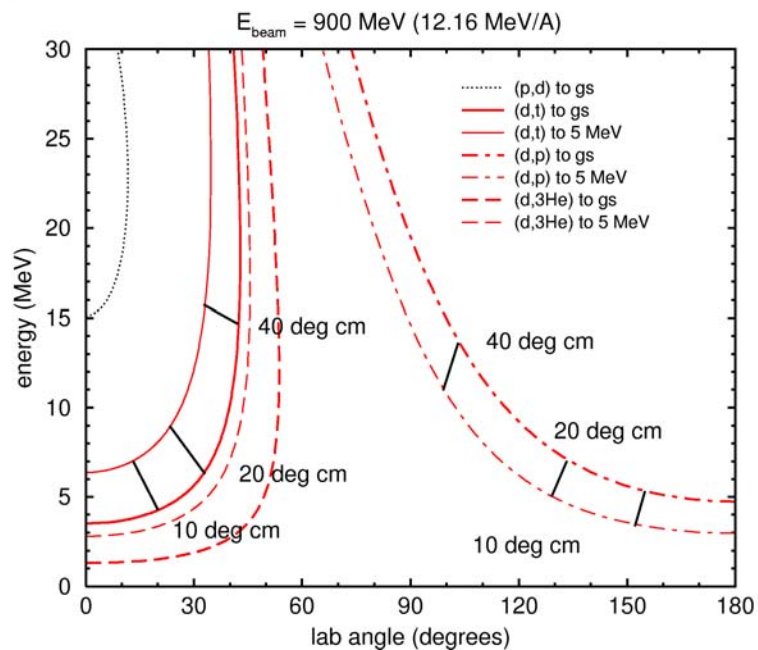
⁷²Kr at 15 MeV/A on p and d targets



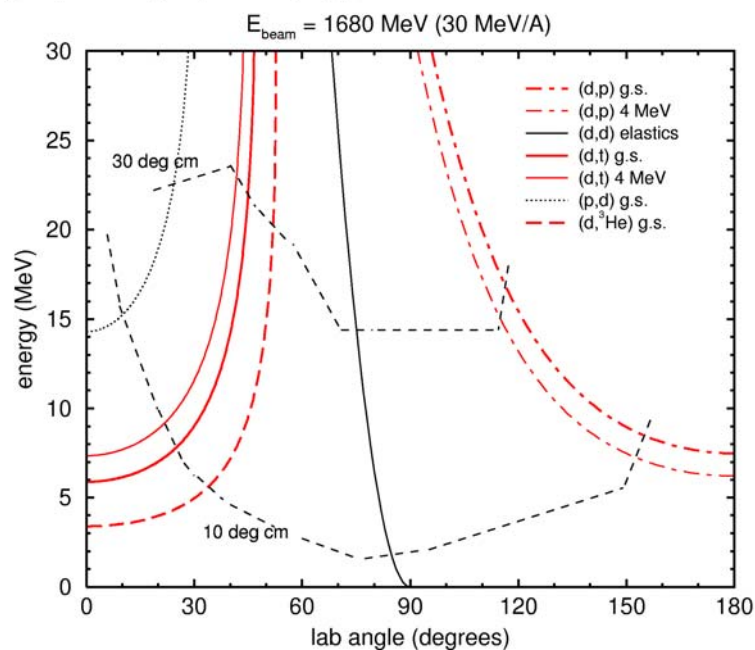
⁷²Kr at 25 MeV/A on d target



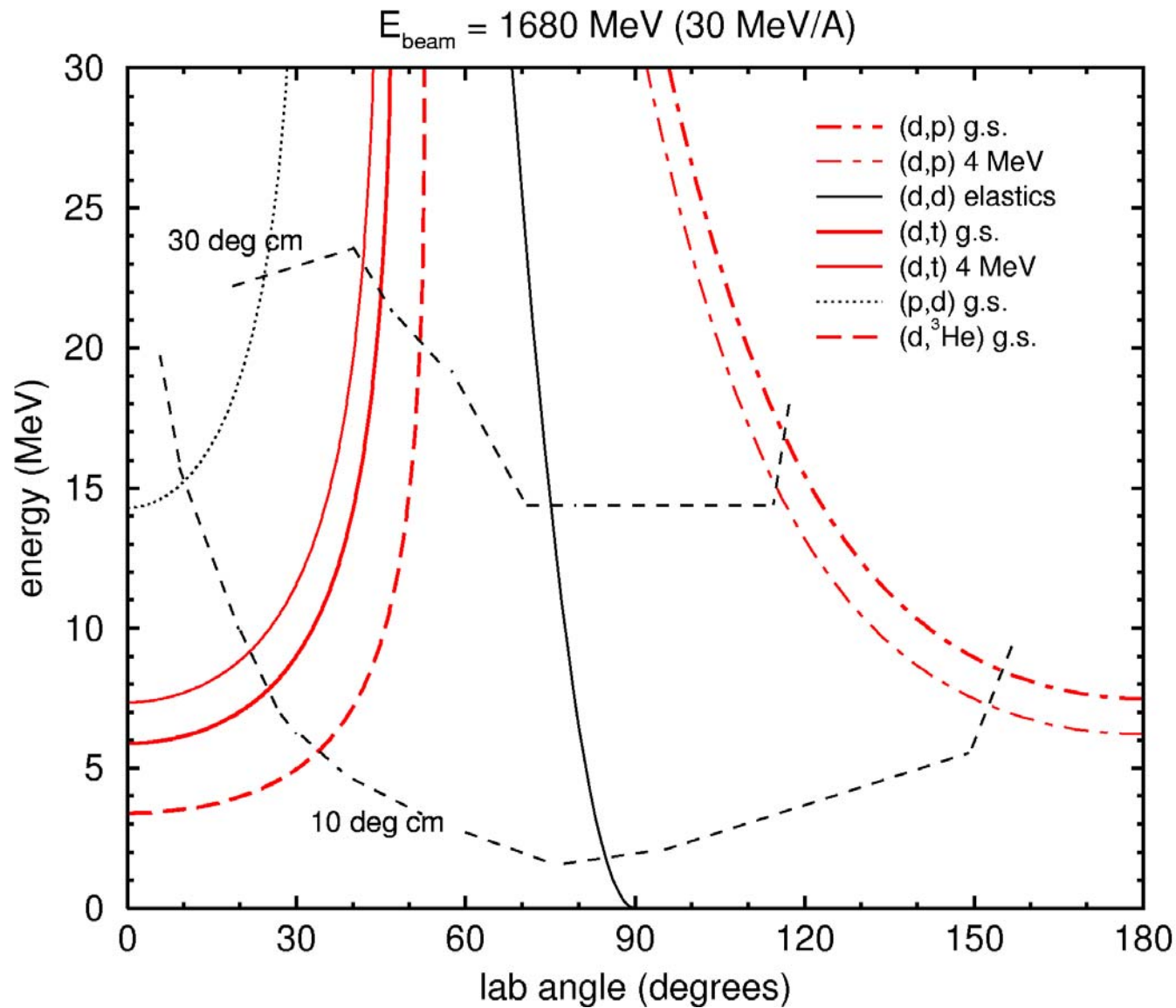
(p,d) and (d,t) and (d,p) on ⁷⁴Kr in inverse kinematics



(p,d) and (d,t) and (d,p) on ⁵⁶Ni in inverse kinematics

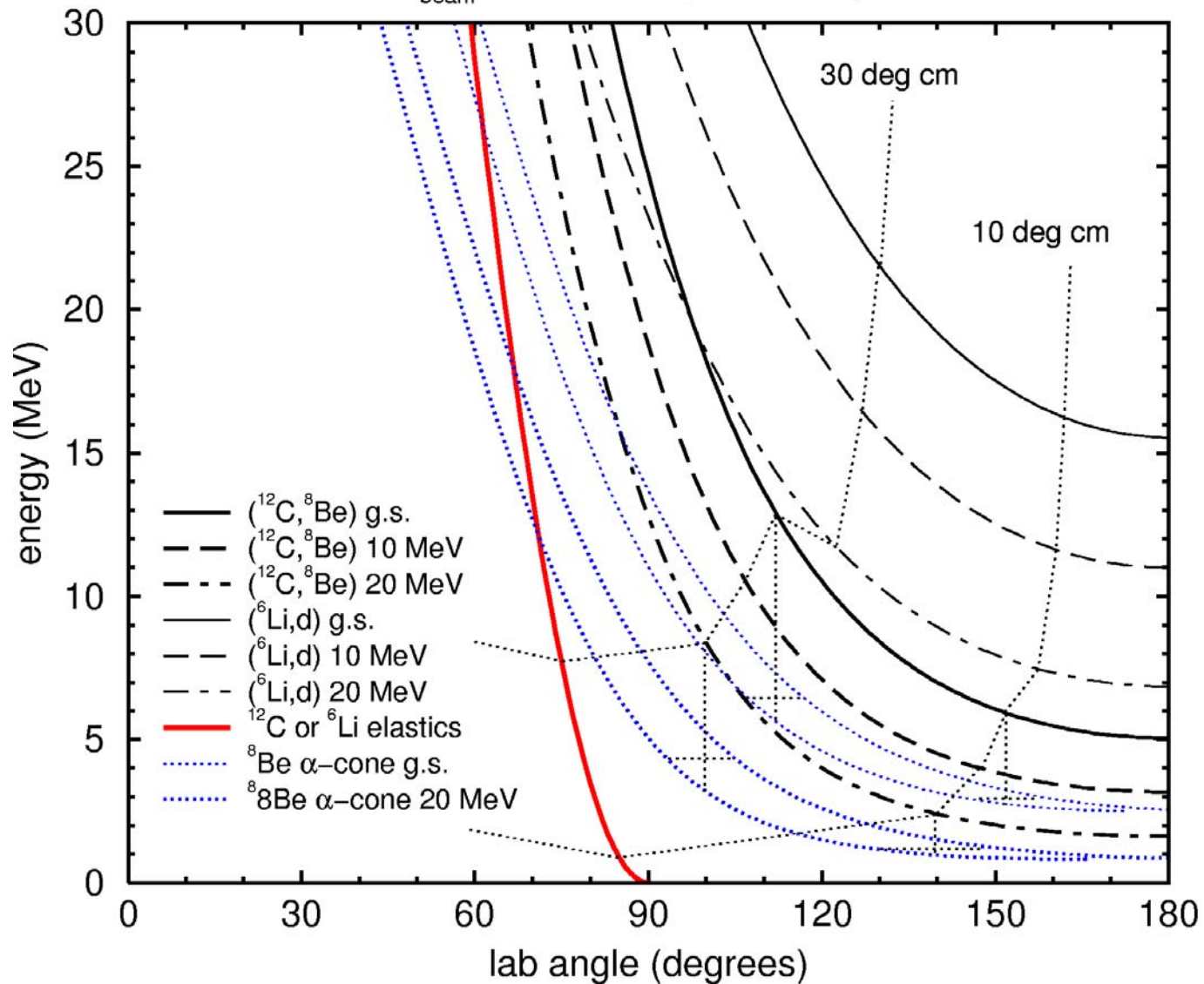


(p,d) and (d,t) and (d,p) on ^{56}Ni in inverse kinematics



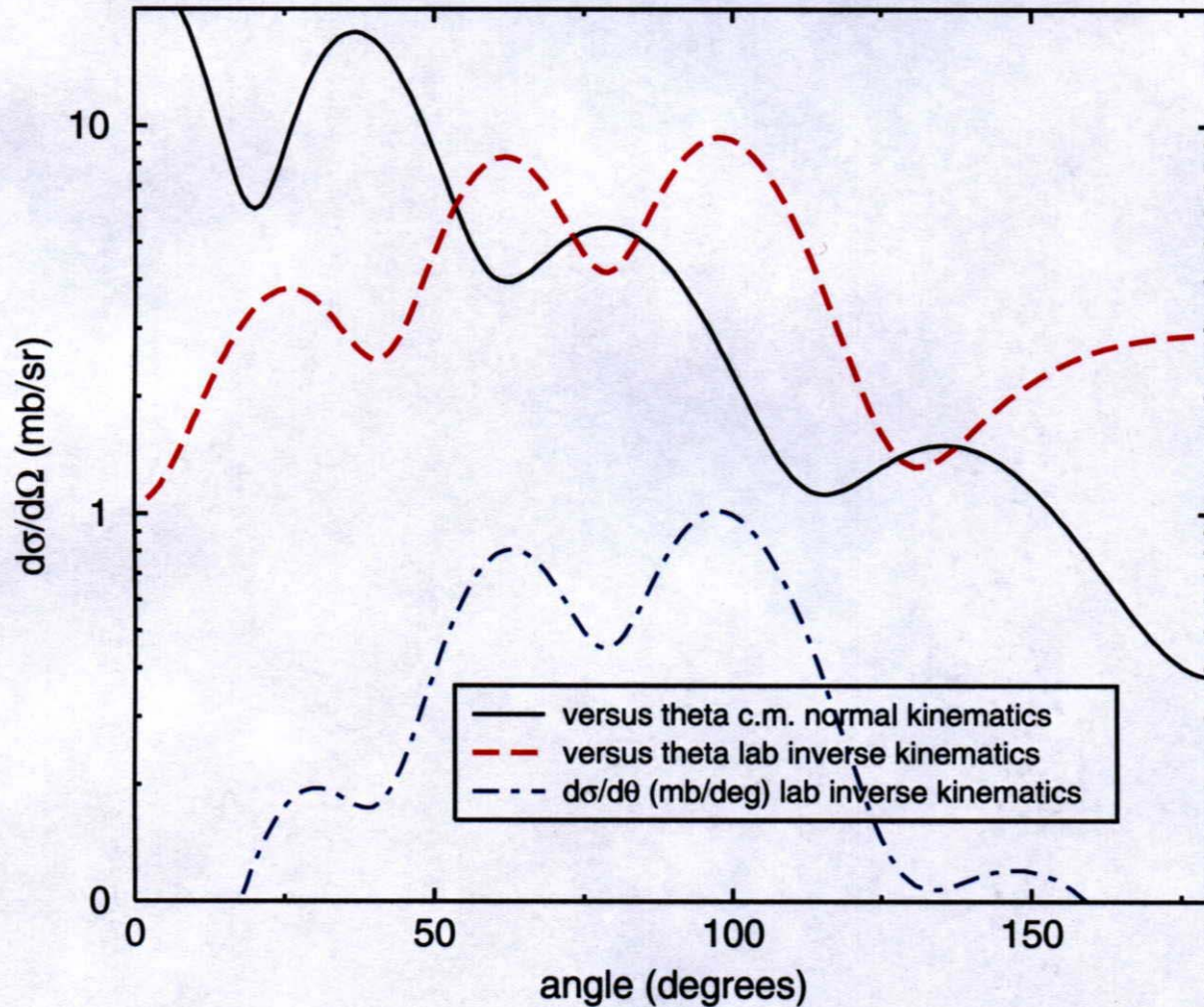
$(^{12}\text{C}, ^8\text{Be})$ and $(^6\text{Li}, d)$ on ^8He in inverse kinematics

$E_{\text{beam}} = 120 \text{ MeV (15 MeV/A)}$



DWBA ZR: $^{94}\text{Sr}(d,p)^{95}\text{Sr}^*(1.0\text{MeV};s_{1/2})$ at 4.894 MeV/u

Adiabatic deuteron potential (B-G) and Perey proton potential



Calculations of E_x resolution from particle detection

152

J.S. Winfield et al. / Nucl. Instr. and Meth. in Phys. Res. A 396 (1997) 147–164

Table 2

Major contributions in keV to the resolution of the excitation energy spectra of single neutron stripping and pickup reactions in inverse kinematics, where the heavy ion is detected in a spectrometer. The detection angle corresponds to 10°_{cm} . The last column is an approximate estimate as a sum in quadrature of the net effect of five non-Gaussian contributions. Other symbols are explained in the text

Reaction	E_i/A (MeV)	θ_{lab}	Origin of contribution					Σ_{quad}
			$\Delta\theta$	Δp	E_{stragg}	$\Theta_{1/2}$	dE/dx	
$p(^{12}\text{Be}, ^{11}\text{Be})d$	30	1.07°	172	147	101	74	23	259
$p(^{12}\text{Be}, ^{11}\text{Be})d$	15	1.06°	84	71	99	74	37	169
$p(^{77}\text{Kr}, ^{76}\text{Kr})d$	30	0.16°	1404	811	808	723	56	1952
$p(^{77}\text{Kr}, ^{76}\text{Kr})d$	10	0.10°	334	143	502	570	268	883
$d(^{76}\text{Kr}, ^{77}\text{Kr})p$	10	0.21°	1140	614	2177	1859	1321	3408

beamlike
particle
detected

Table 3

Major contributions in keV to the resolution of the excitation energy spectra of single neutron pickup and stripping reactions in inverse kinematics, where the light particle is detected in a silicon detector. Symbols as described in text and Table 2

Reaction	E_i/A (MeV)	θ_{lab}	Origin of contribution					Σ_{quad}
			$\Delta\theta$	ΔE_f	ΔE_i	$\Theta_{1/2}$	dE/dx	
$p(^{12}\text{Be}, d)^{11}\text{Be}$	30	19.0°	136	74	114	96	649	685
$p(^{12}\text{Be}, d)^{11}\text{Be}$	15	17.8°	66	72	55	89	984	995
$p(^{77}\text{Kr}, d)^{76}\text{Kr}$	30	15.0°	124	55	64	63	186	249
$p(^{77}\text{Kr}, d)^{76}\text{Kr}$	10	6.0°	26	24	23	19	775	777
$d(^{76}\text{Kr}, p)^{77}\text{Kr}$	10	155.3°	52	93	37	60	1309	1316

light
particle
detected

Lighter projectiles

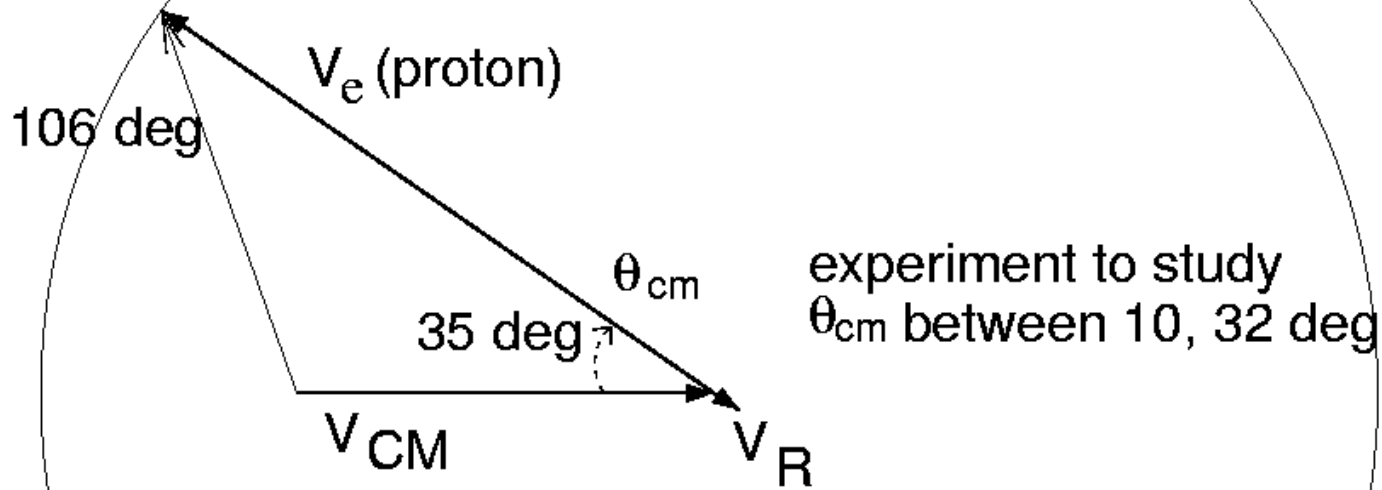
Some advantages to detect beam-like particle
(gets difficult at higher energies)

Heavier projectiles

Better to detect light particle
(target thickness limits resolution)



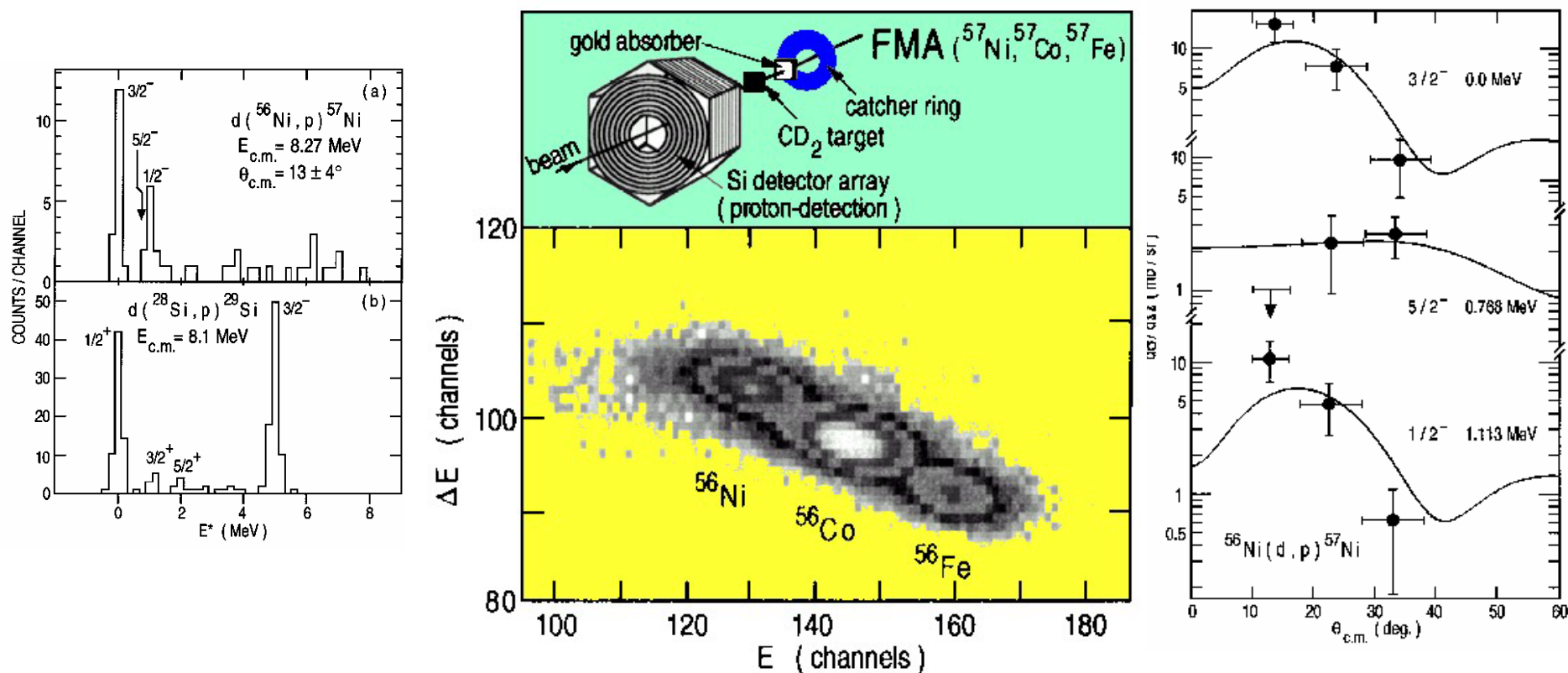
4.0 MeV/A
 (~24MV 15+)
 376 MeV

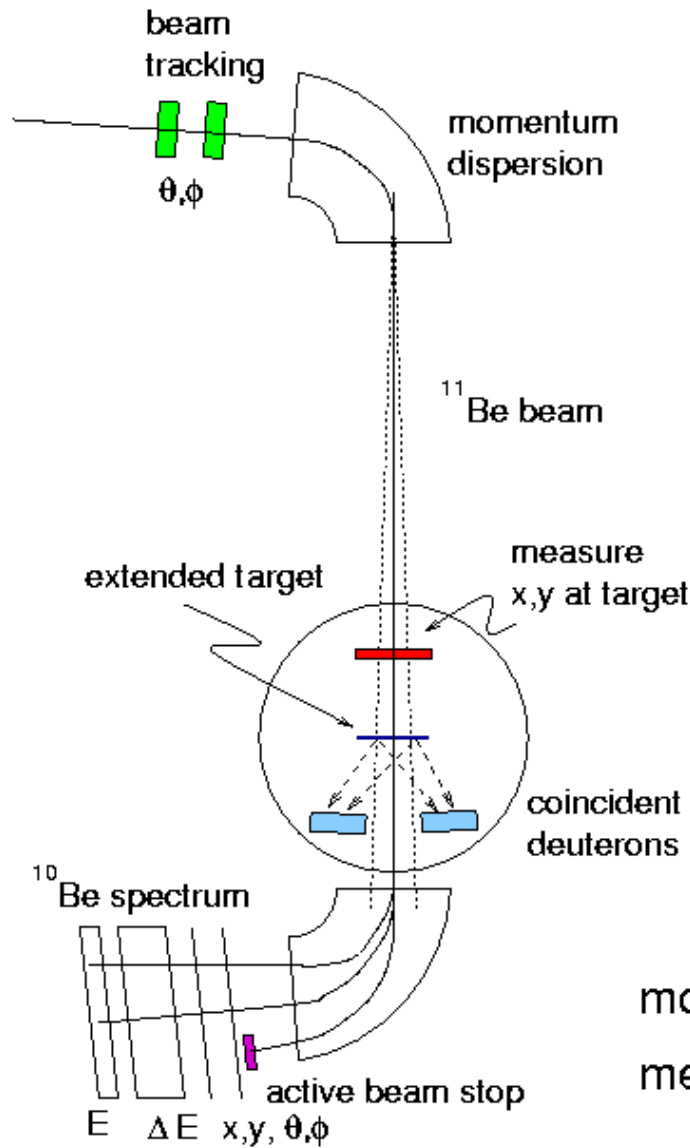
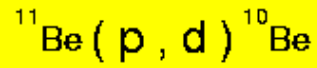


θ_{lab}	θ_{cm}	E_{proton}	0.2 deg $\Delta\theta$	35 keV E_{res}	ENRGY STRAG	MULT/ SCATT	DIFF'L DE/DX TARG	TOTAL IN QUAD	DE(Ex) /DE(Ep)
112	32	3.33	23	50	19	56	393	401	-1.43
154	10	1.58	7	87	21	23	389	400	-2.53

Study of the $^{56}\text{Ni}(d,p)^{57}\text{Ni}$ Reaction and the Astrophysical $^{56}\text{Ni}(p,\gamma)^{57}\text{Cu}$ Reaction Rate

K. E. Rehm,¹ F. Borasi,¹ C. L. Jiang,¹ D. Ackermann,¹ I. Ahmad,¹ B. A. Brown,² F. Brumwell,¹ C. N. Davids,¹
 P. Decroock,¹ S. M. Fischer,¹ J. Görres,³ J. Greene,¹ G. Hackmann,¹ B. Harss,¹ D. Henderson,¹ W. Henning,¹
 R. V. F. Janssens,¹ G. McMichael,¹ V. Nanal,¹ D. Nisius,¹ J. Nolen,¹ R. C. Pardo,¹ M. Paul,⁴ P. Reiter,¹ J. P. Schiffer,¹
 D. Seweryniak,¹ R. E. Segel,⁵ M. Wiescher,³ and A. H. Wuosmaa¹





beam energy
resolution 2.0-3.0 MeV

angular spread $\pm 1^\circ$

dispersion-matched spectrometer "SPEG"
(Spectromètre à Perte d'Énergie du Ganil)

microchannel plate

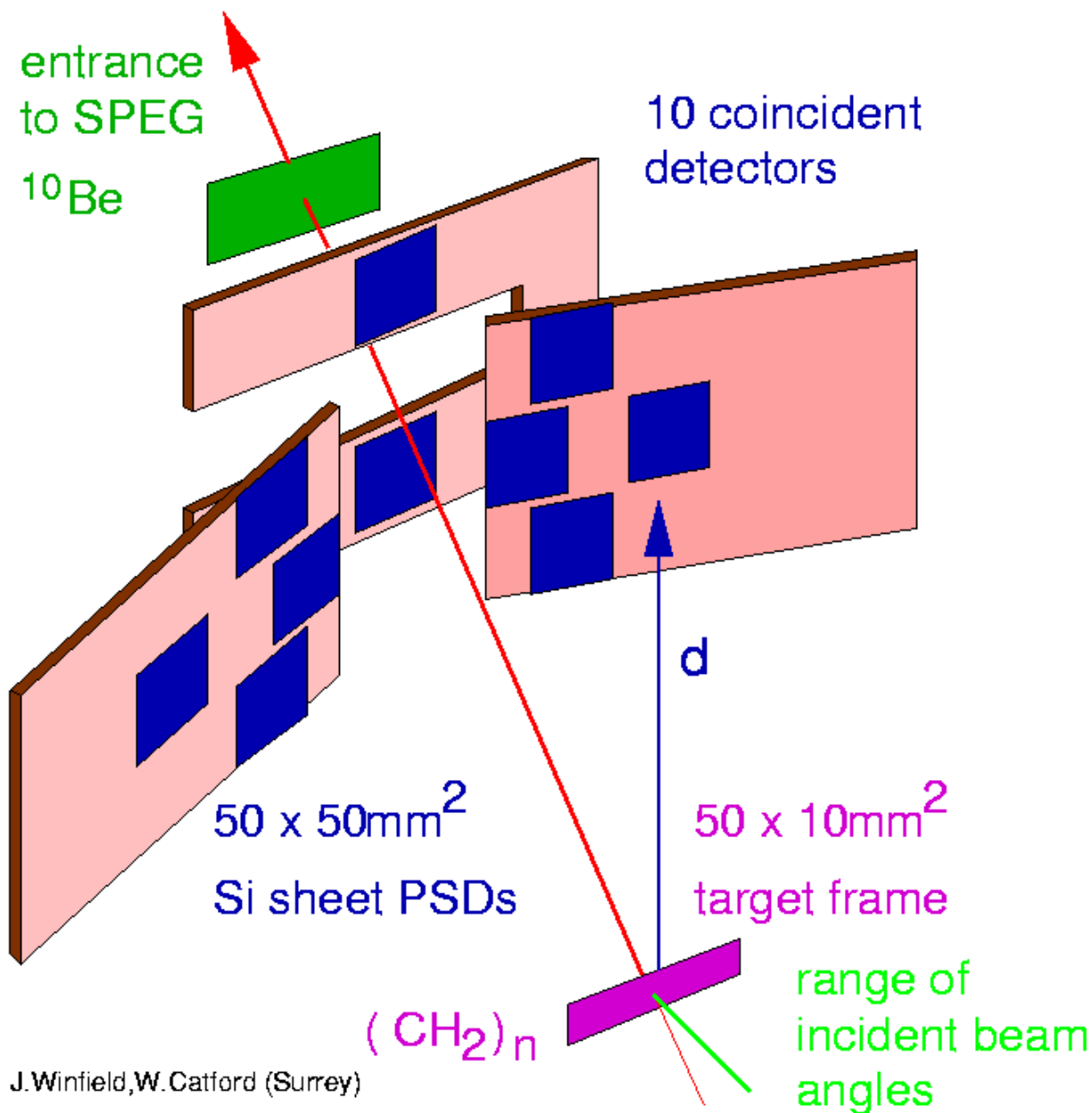
polythene target

ten Silicon PSD's

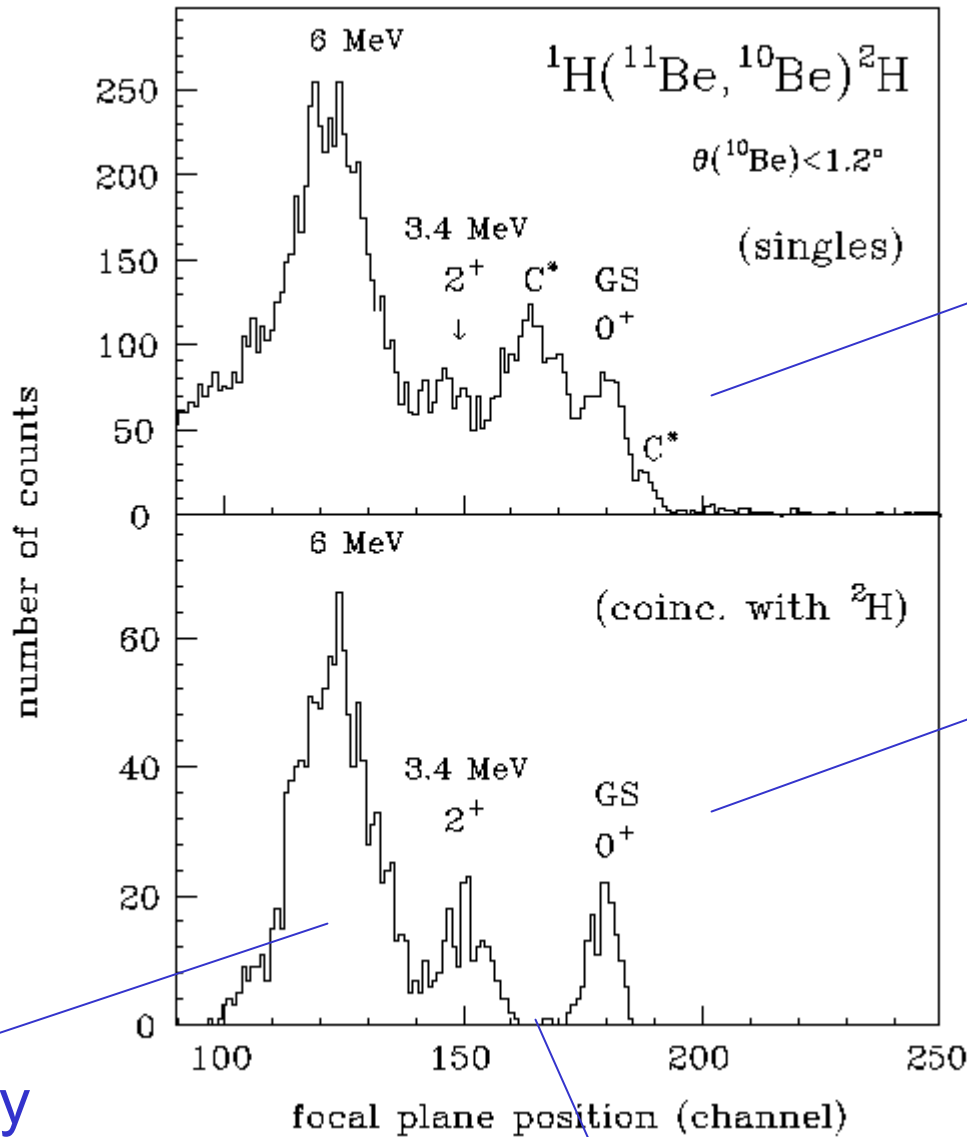
momentum analysis
measure reaction angle

^{10}Be spectrum
E ΔE x,y, θ, ϕ
active beam stop

Inverse kinematics ^{11}Be (p,d) ^{10}Be



Focal plane spectrum from SPEG magnetic spectrometer



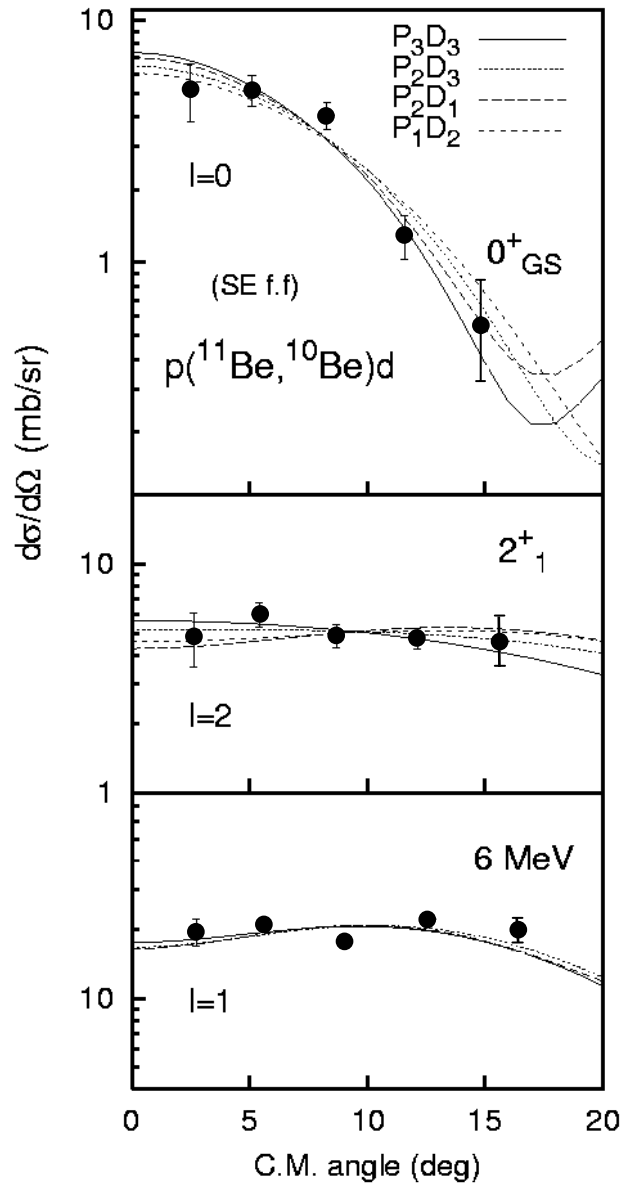
singles

coincidence

gamma-ray
broadening

carbon background removed

Separation Energy form factor



0^+ 2^+
 α^2 β^2

~~0.49 0.51~~

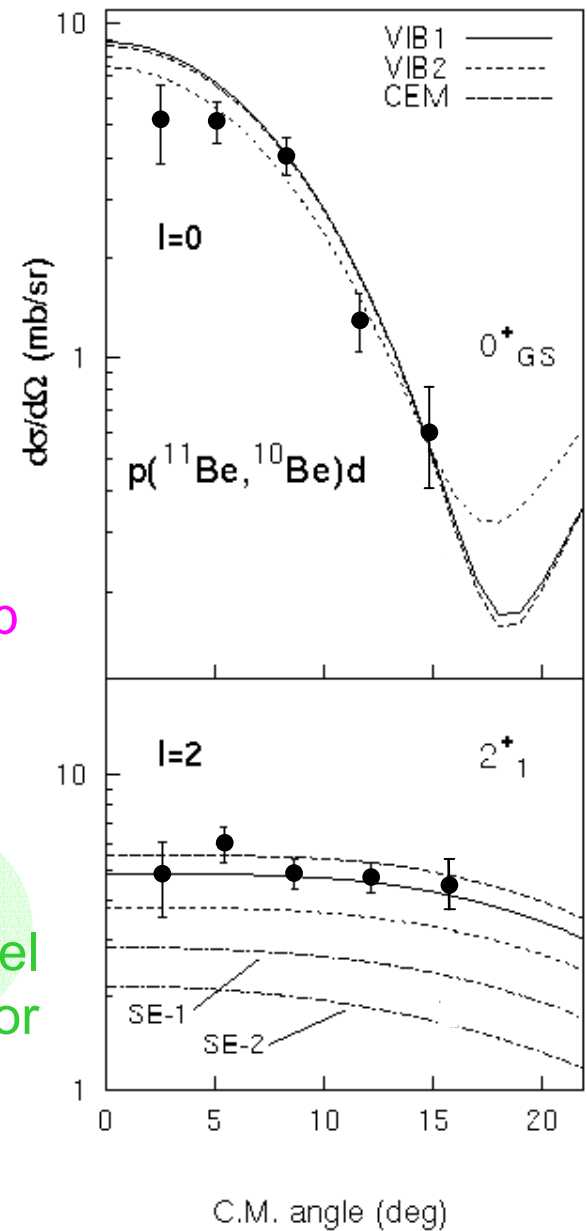
- poor form factor
- no core coupling
- no $^{11}\text{Be}/d$ breakup

0.84 0.16

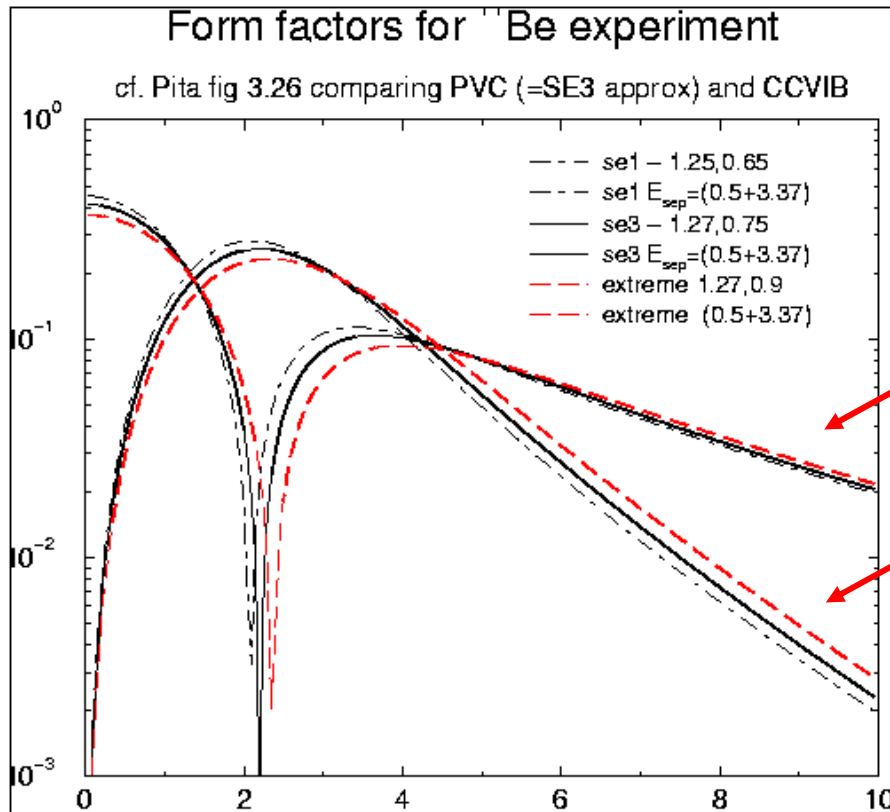
- vibrational model
- core-excited model
- realistic form factor

$\left\{ \begin{array}{cc} 0.74 & 0.19 \\ \text{Shell model} \end{array} \right\}$

Vibrational form factor



Radial form factor for the transferred nucleon (in ^{11}Be)



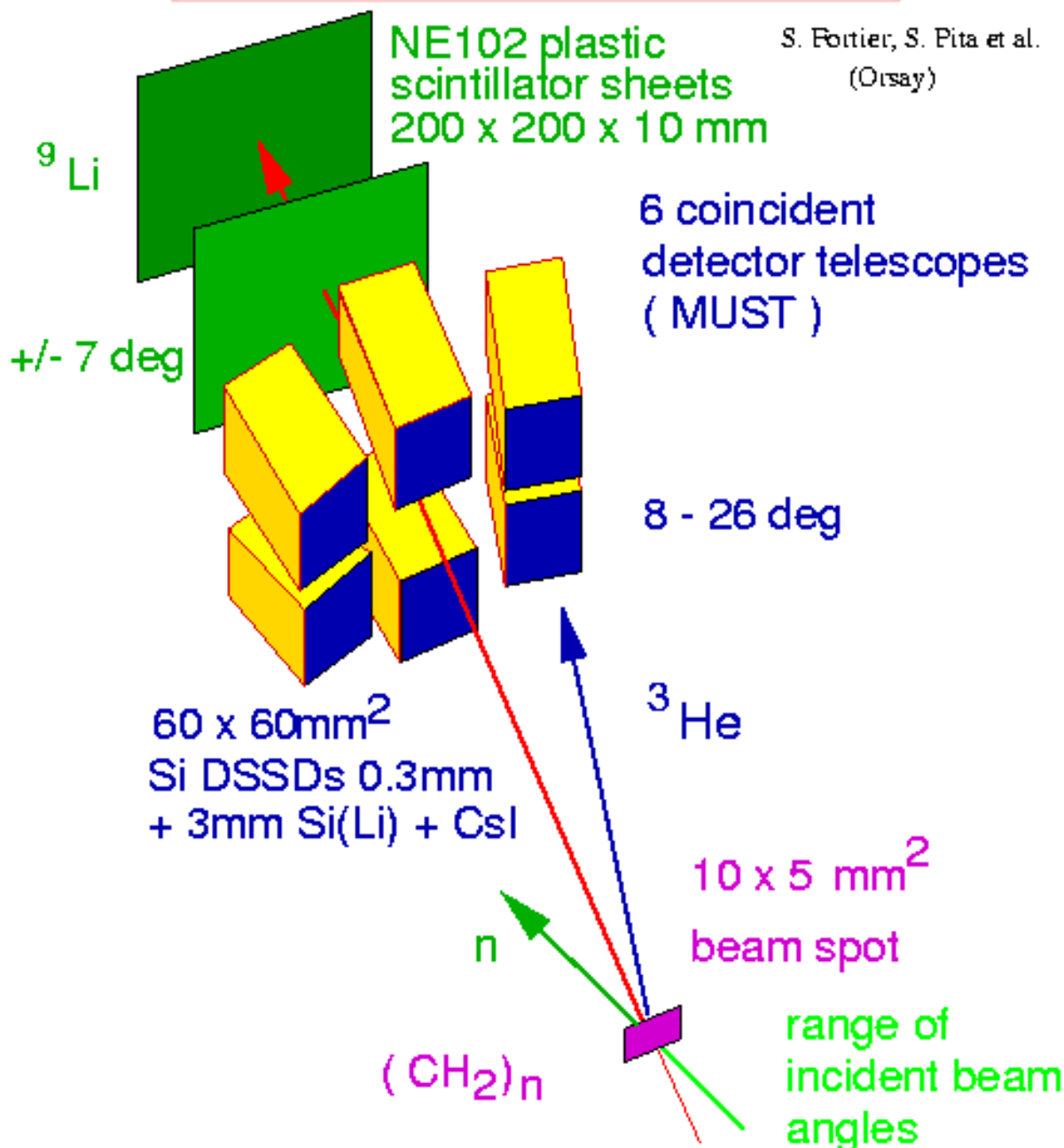
s-wave bound state wfn

d-wave bound state wfn

The relative magnitudes of the s- and d-wave form factors can be changed by **changing the potential geometry** OR by using a **core excitation model** and solving the coupled equations. The two have subtly different effects

Inverse kinematics $^{11}\text{Be}(d, ^3\text{He})^{10}\text{Li}$

S. Fortier, S. Pita et al.
(Orsay)



Excitation energy spectra from the Orsay experiment

S. Fortier,
S. Pita et al.,
(2000)

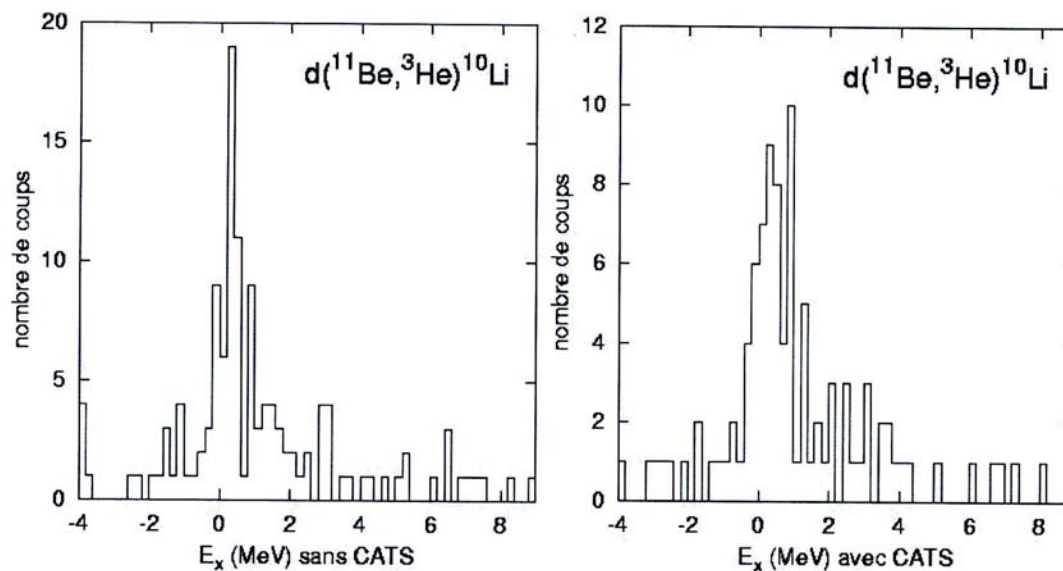


Figure 4.16: spectres en énergie du ^{10}Li , obtenus sans CATS (gauche) et avec CATS (droite)

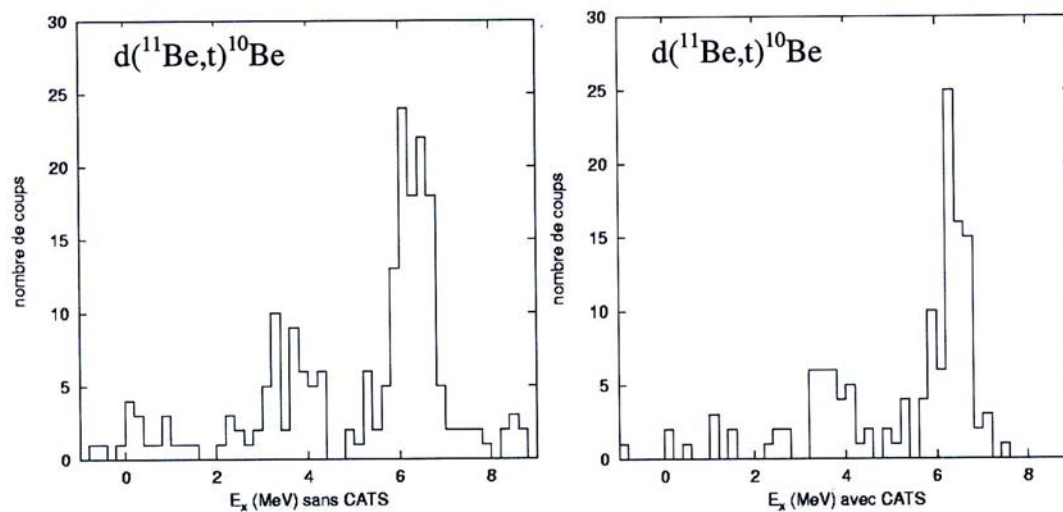
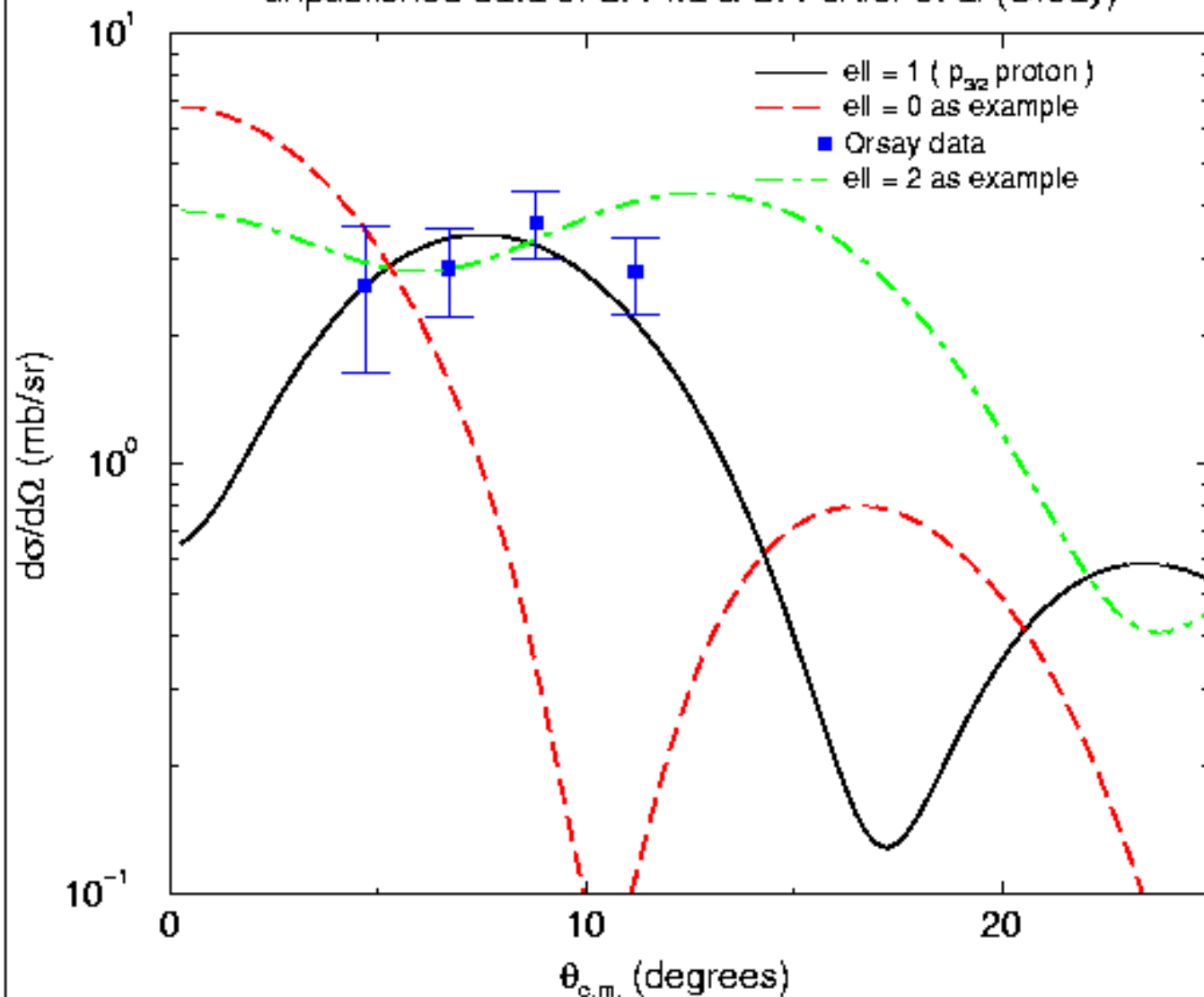


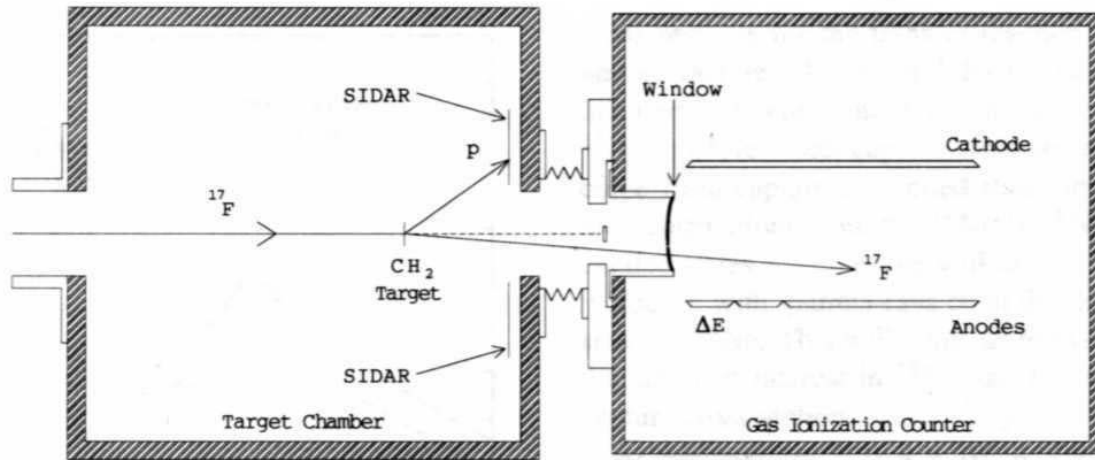
Figure 4.17: spectres d'énergie d'excitation du ^{10}Be obtenus sans (gauche) et avec (droite) les détecteurs CATS.

Results from $d(^7\text{Be}, ^7\text{He})^7\text{Li}$ at 37.3 MeV/A

unpublished data of S. Pita & S. Fortier et al (Orsay)



Resonance scattering at ORNL: $^{18}\text{F} (p, \alpha) ^{15}\text{O}$



$$E_{\text{beam}} = 0.65 \text{ MeV/A}$$

$$\theta_{\text{lab}} (\text{Si}) = 15 - 45^\circ$$

$$Q = + 2.88 \text{ MeV}$$

$$q = 5.563 \gg 1$$

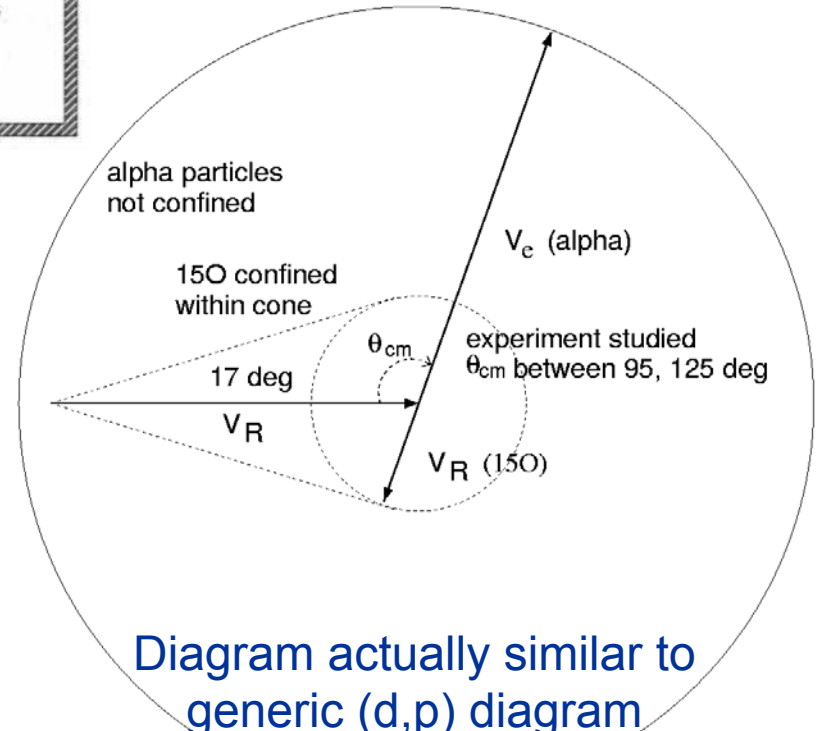
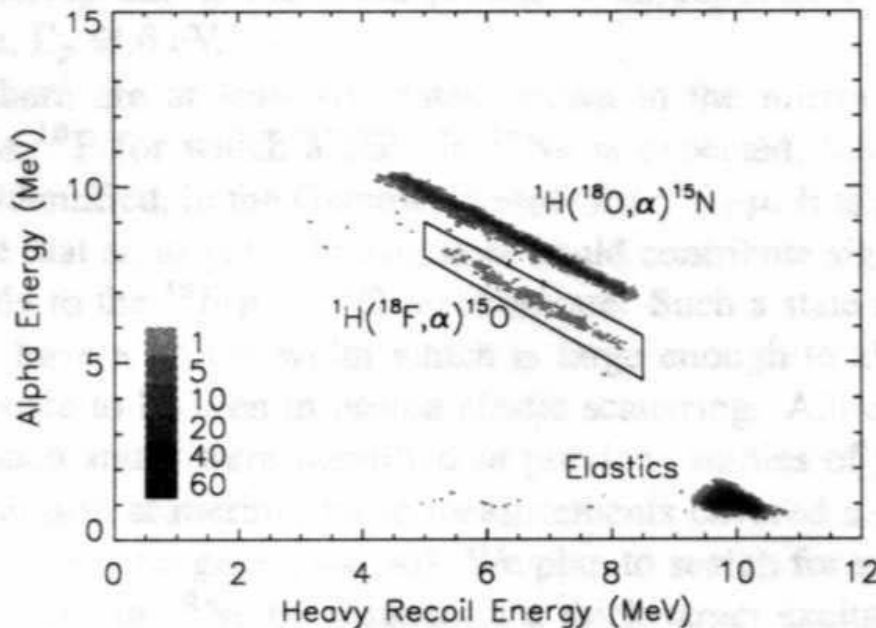


Diagram actually similar to generic (d,p) diagram

(Note: low E/A compared to Q)

Angle and energy of light particle crucial for resolution

Possible Experimental Approaches to Nucleon Transfer

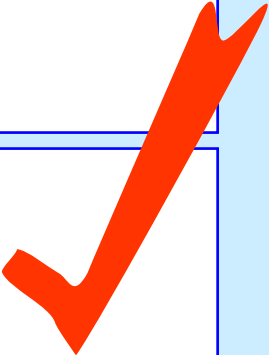
1) Rely on detecting the beam-like ejectile in a spectrometer

- Kinematically favourable unless beam mass (and focussing) *too* great
- Spread in beam energy (several MeV) translates to E_x measurement
- Hence, need energy tagging, or a dispersion matching spectrometer
- Spectrometer is subject to broadening from gamma-decay in flight

2) Rely on detecting the target-like ejectile in a Si detector

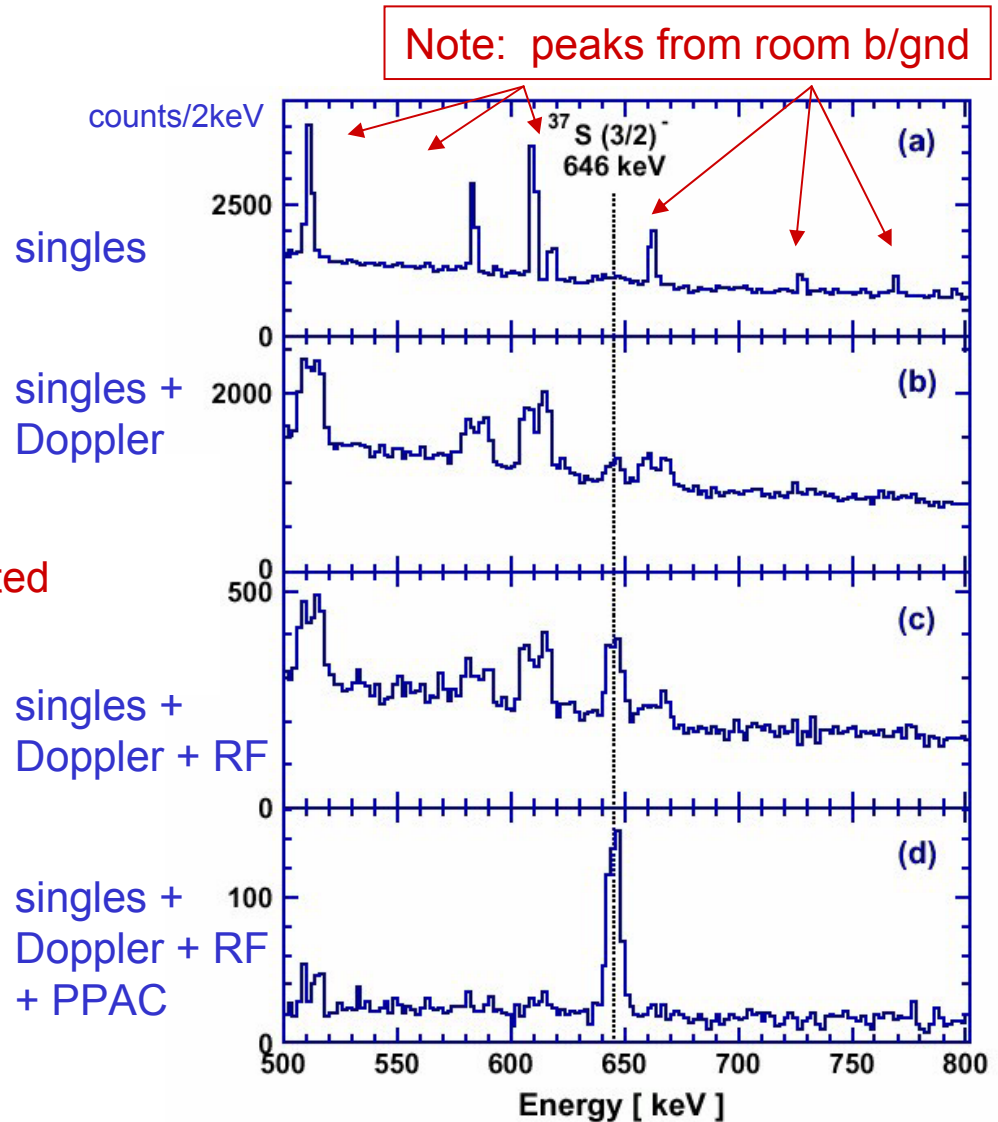
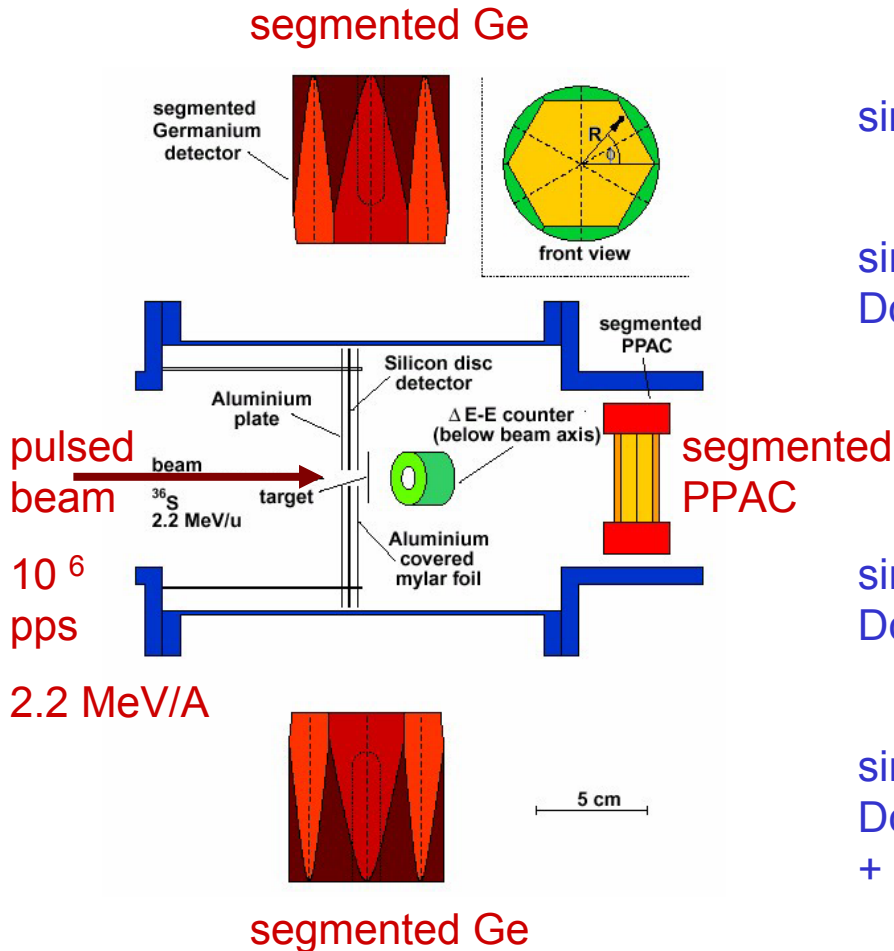
- Kinematically less favourable for angular coverage
- Spread in beam energy generally gives little effect on E_x measurement
- Resolution limited by difference [$dE/dx(\text{beam}) - dE/dx(\text{ejectile})$]
- Target thickness limited to 0.5-1.0 mg/cm² to maintain resolution

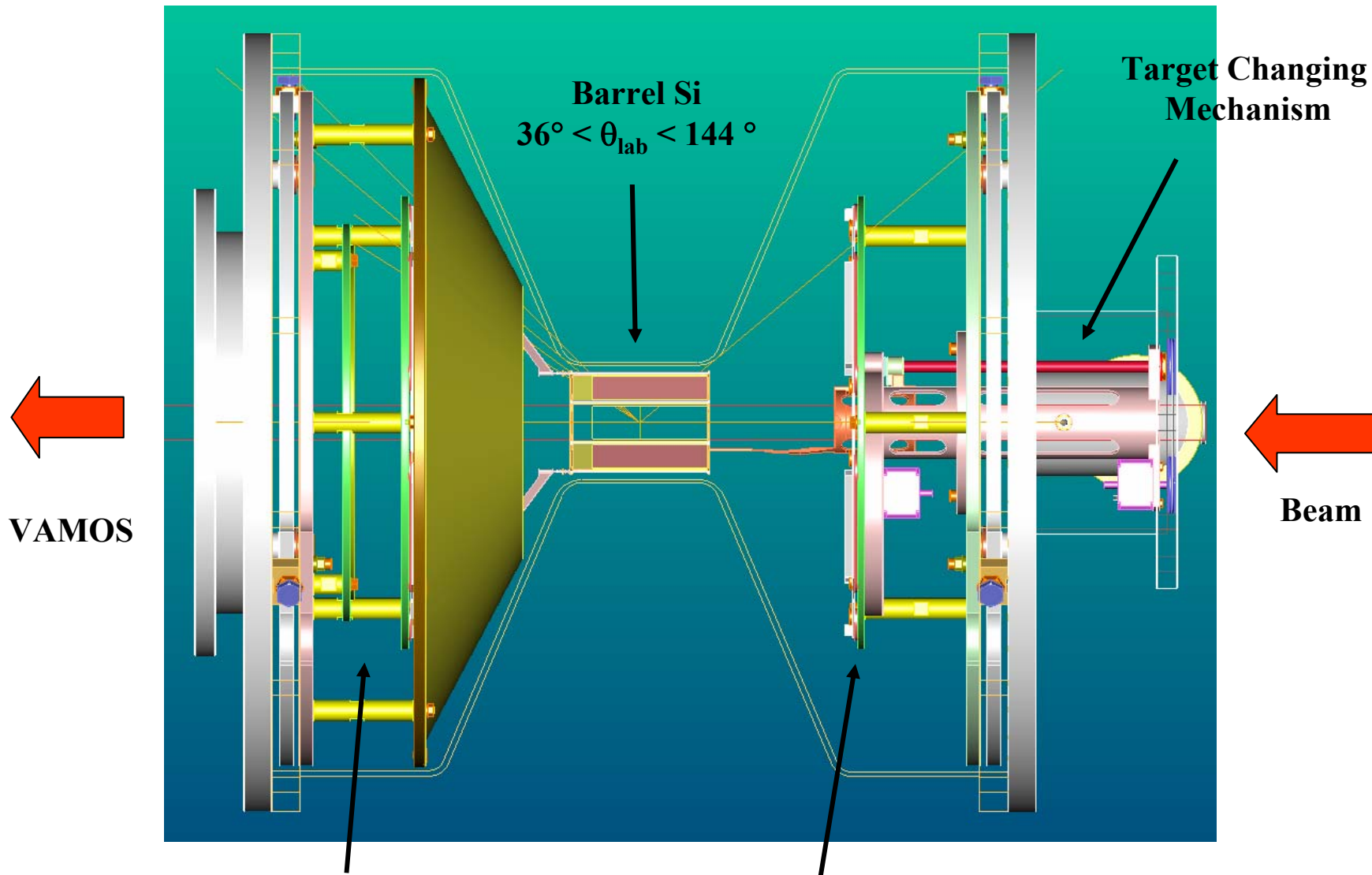
3) Detect decay gamma-rays in addition to particles

- Need exceptionally high efficiency, of order $> 25\%$
 - Resolution limited by Doppler shift and/or broadening
 - Target thickness increased up to factor 10 (detection cutoff, mult scatt'g)
- 

Proof of Principle using weak ^{36}S beam and inverse $^{36}\text{S}(d,p)^{37}\text{S}$

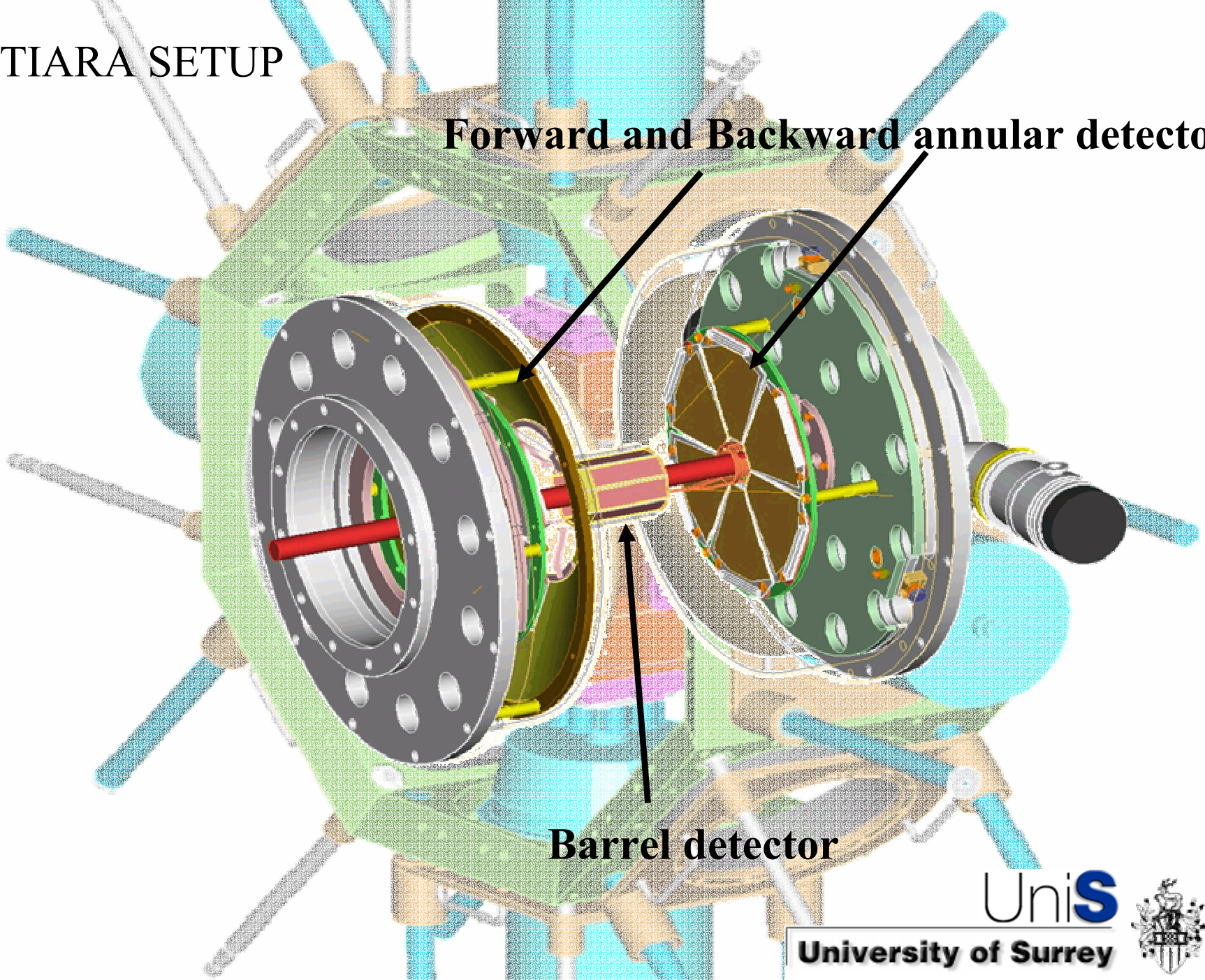
C. Grund *et al.* (Heidelberg/Darmstadt)
 Eur. Phys. J. A10 (2001) 85



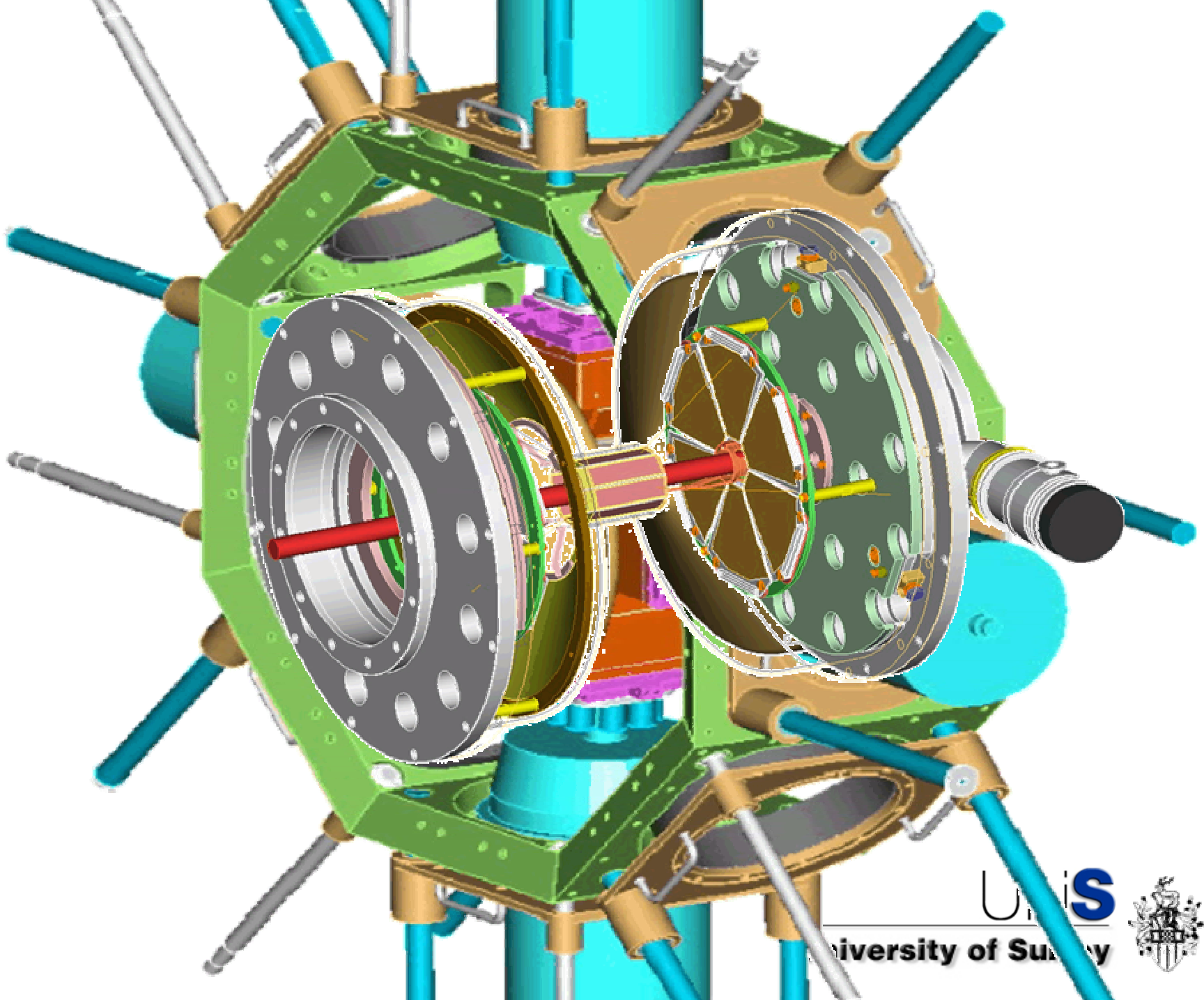


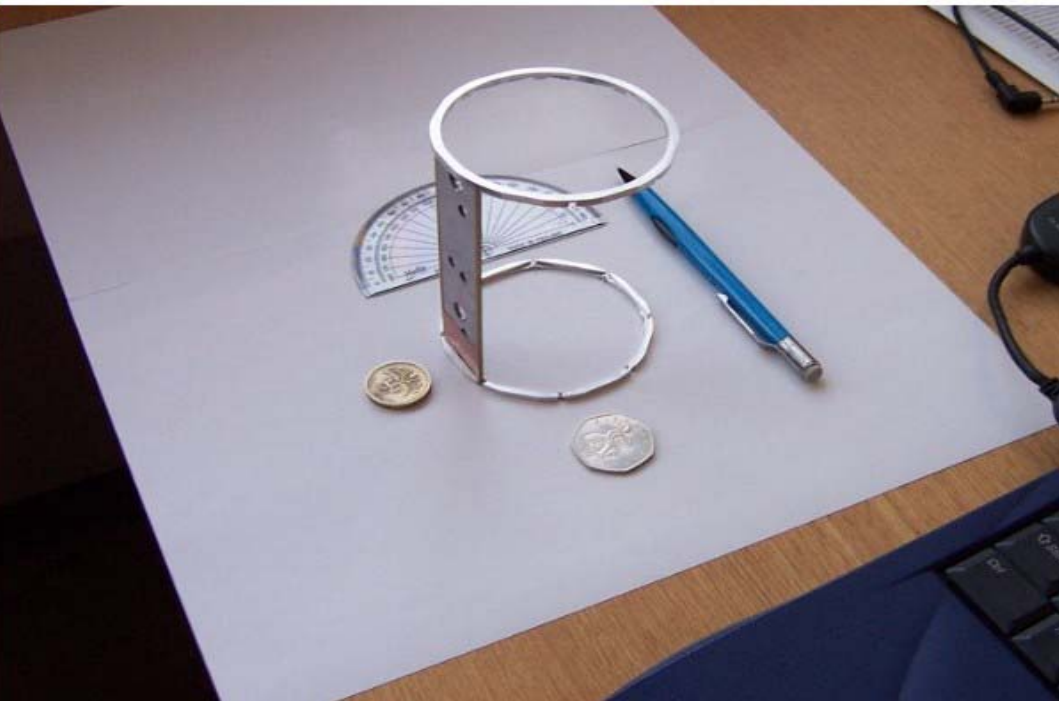
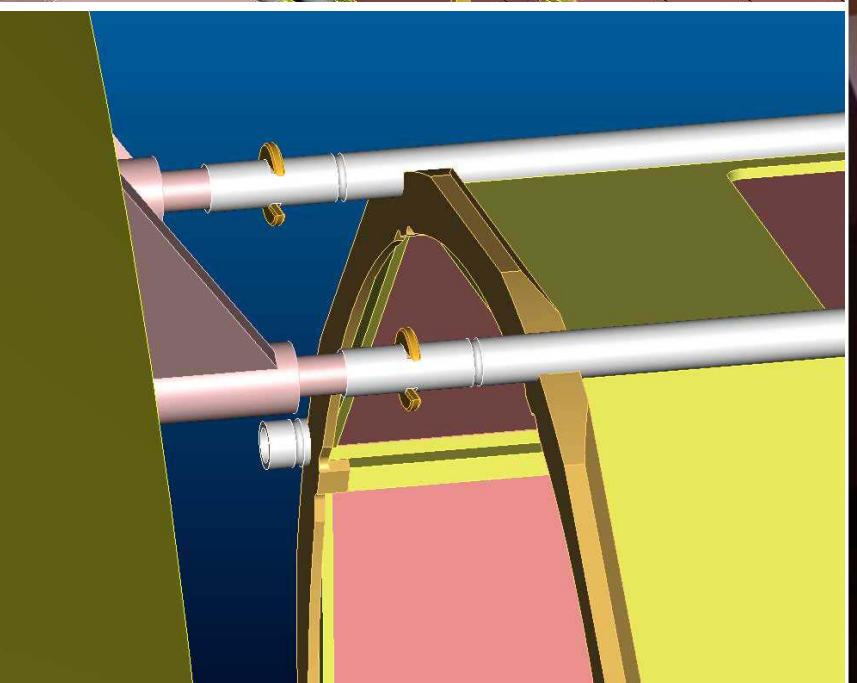
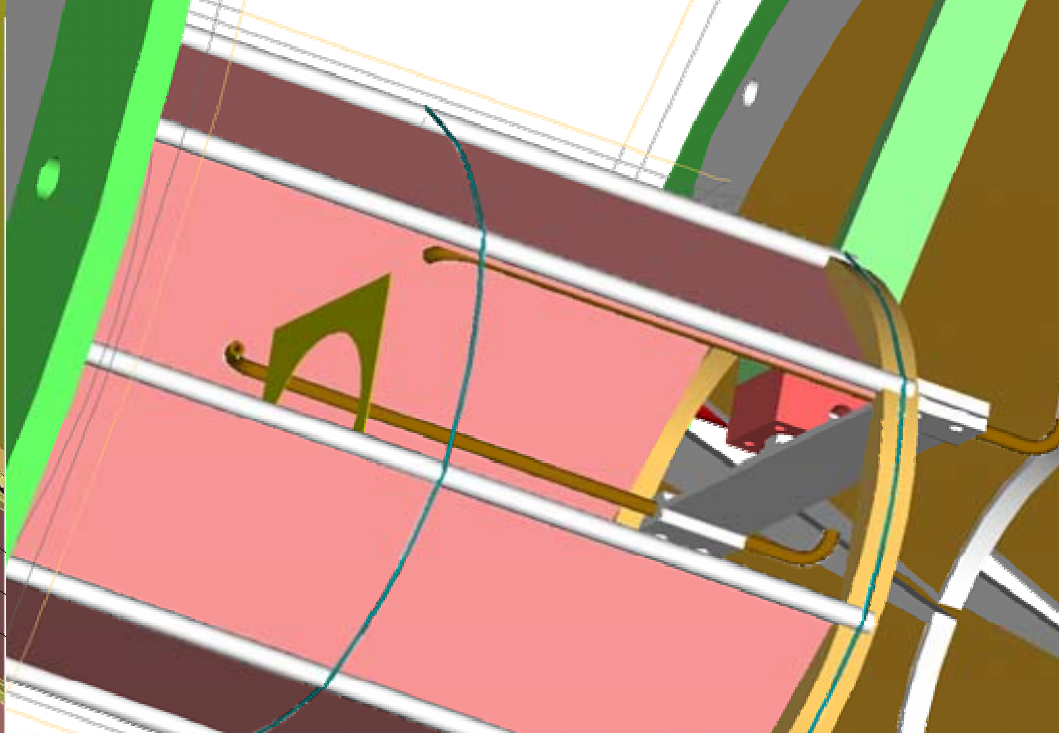
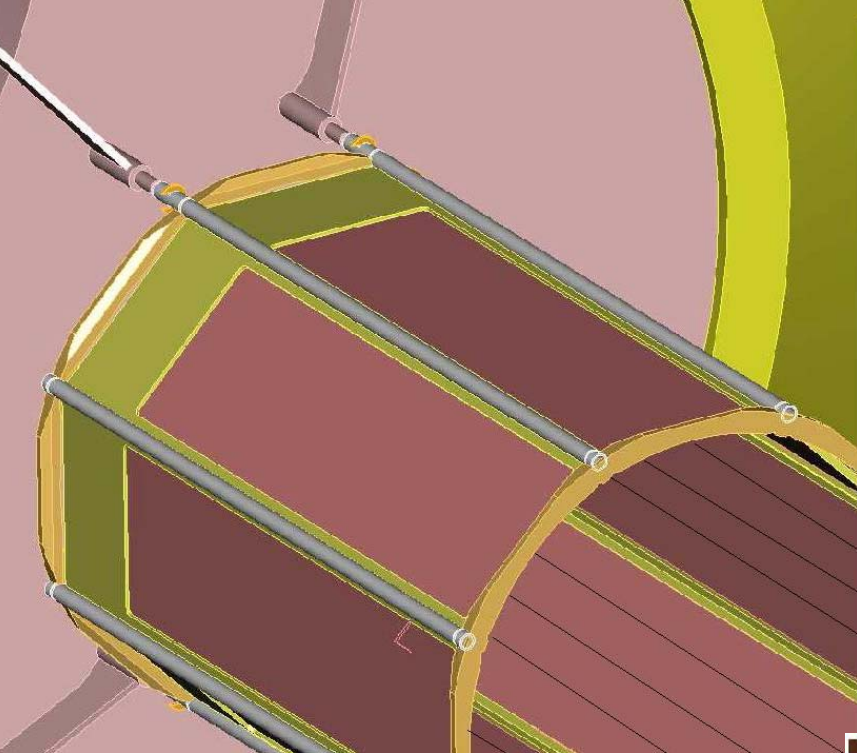
TIARA SETUP

Forward and Backward annular detectors



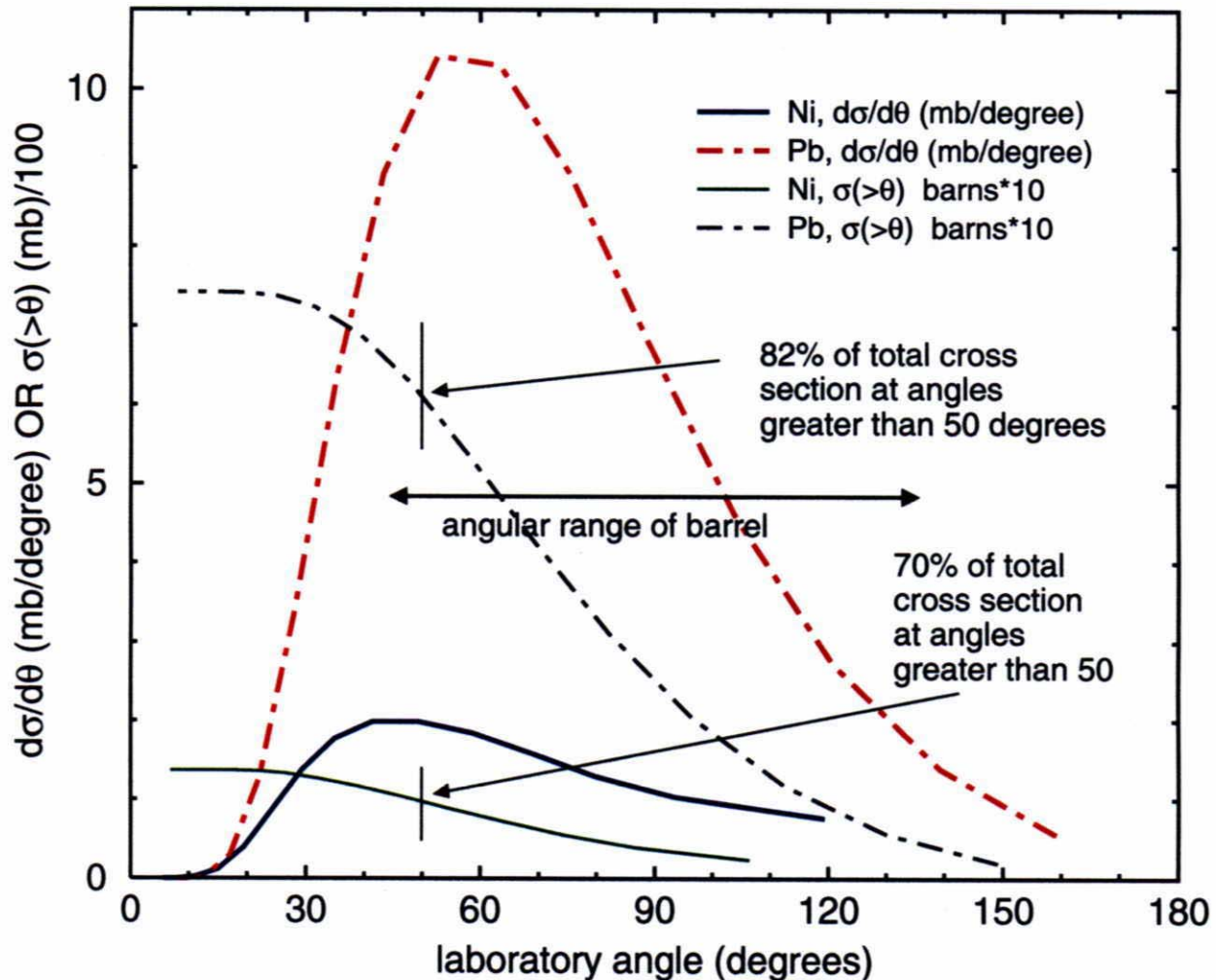
Barrel detector





Coulex of ^{46}Ar (2^+ ; 1.577 MeV) , Ni & Pb targets

$B(E2)=196 e^2\text{fm}^4$; safe energies of 90 MeV (Ni) and 155 MeV (Pb)



OUTLOOK

Experimentally proven

- *inverse kinematics manageable*
- *gamma-ray detection often desirable*

Reactions on p and d targets

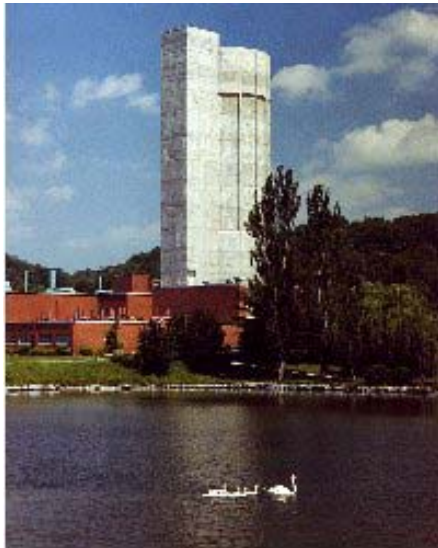
- *identify angular momentum and E_x*
- *then, measure spectroscopic factors*

Alpha 2-nucleon transfer

- *(d, ^6Li) or (^{12}C , ^8Be) or (^6Li , d) possible*
- *(t, p) or (^9Be , ^7Be) or (^{10}B , ^8B) possible*

Experimental challenges

- *pushing beyond 35-40 deg in (p, d) etc.*
- *stopping all particles & detecting gammas*
- *low energy thresholds for particles*
- *detection of beam-like particle (identify Z)*
- *scattered beam particles are radioactive*



Oak Ridge TN
June 2002